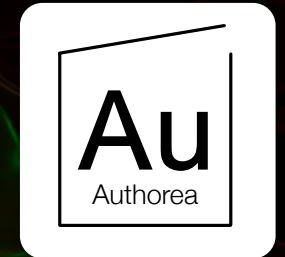
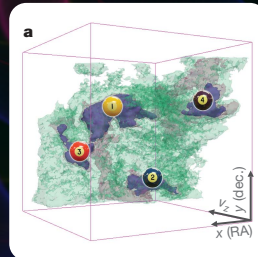
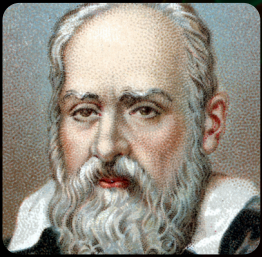


THE VALUE OF HIGH-DIMENSIONAL DATA VISUALIZATION IN SCIENCE

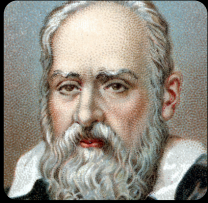


Alyssa A. Goodman

*Harvard-Smithsonian Center for Astrophysics
& Radcliffe Institute
@aagie*

Thomas Robitaille

*lead Developer for glue
@astrofrog*



IN GALILEO'S MIND'S EYE



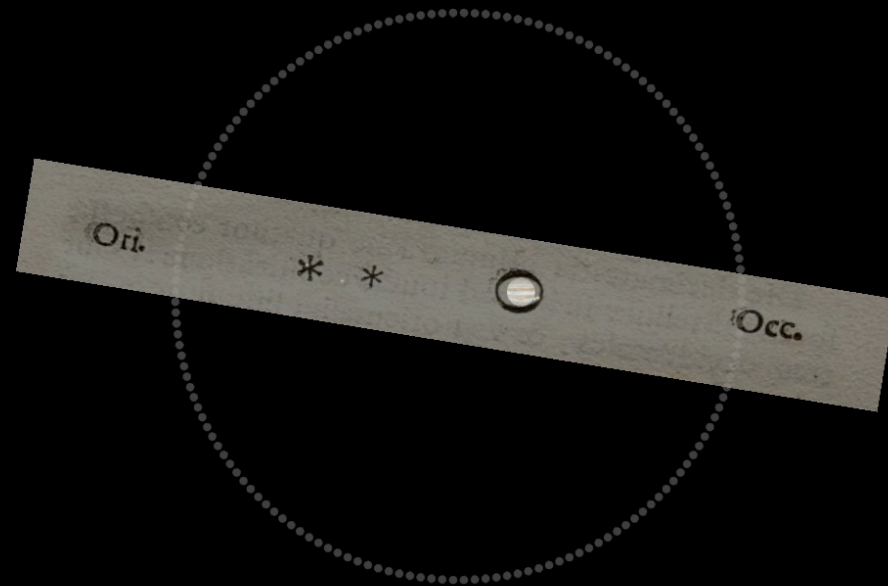
Sex^{to} Principe.

Galileo Galilei, Familij. Senus della Ser.^a V. inuigilantissimo, et de ogni spirito se bene no solum satisfare alvario che non della Lettera di Mathematici nella Scuola di Padova,

Inuere deueno determinato di presentare al Sex^{to} Principe l'Orbicle et il p^{ro}posito di giuamento inestimabile di ogni regio et in linea marittima o terrestre sicut di tenere pulito nuovo artificio ne l' maggior segreto et solam a disposizione di o^{ro} Ser.^a L' Orbicle canato dalle piu^e di dite speculationi di pros^o bottona ne l' vantaggio di scoprire Legni et Vele dell' inimici di Vae hore et piu di tempo prima che essi scuopra noi et distinguendo il numero et la qualita de i Vesselli giudiare li sue forze pallestris alla caccia al ambramento o alla fuga, o fare essi nella campagna aperta in esse et particolarly Distinguerli ogni suo moto et propriamento.

Offe. 7. di gennaio
 Giove si vede a^o 10. 11.
 Ahi 8. ahi
 Ahi 12. si vede in tale costellazione
 Il 13. si vedono minime a Giove 4 stelle
 Ahi 14. è angelo
 Il 15. la pros^a a 7. ora in m^o la f. ora di.
 stante dalla 3^a il doppio si era
 Lo spazio delle 3. meridiane ad ora
 maggiore del diametro di 7. et e.
 1000 in linea retta.

January 11, 1610



IN GELLER, HUCHRA & DELAPPARENT'S MINDS' EYES



THE ASTROPHYSICAL JOURNAL, 302:L1-L5, 1986 March 1
 © 1986. The American Astronomical Society. All rights reserved. Printed in U.S.A.

A SLICE OF THE UNIVERSE¹

VALÉRIE DE LAPPARENT,^{2,3} MARGARET J. GELLER,² AND JOHN P. HUCHRA²
 Received 1985 November 12; accepted 1985 December 5

ABSTRACT

We describe recent results obtained as part of the extension of the Center for Astrophysics redshift survey to $m_B = 15.5$. The new sample contains 1100 galaxies (we measured 584 new redshifts) in a $6^\circ \times 117^\circ$ strip going through the Coma cluster. Several features of the data are striking. The galaxies appear to be on the surfaces of bubble-like structures. The bubbles have a typical diameter of $\sim 25h^{-1}$ Mpc. The largest bubble in the survey has a diameter of $\sim 50h^{-1}$ Mpc, comparable with the most recent estimates of the diameter of the void in Bootes. The galaxy density in the region of the largest void contained in the survey is only 0.20 of the mean. The edge of the largest void in the survey is remarkably sharp.

All of these features pose serious challenges for current models for the formation of large-scale structure. The best available model for generating these structures is the explosive galaxy formation theory of Ostriker and Cowie, published in 1981. These new data might be the basis for a new picture of the galaxy and cluster distributions.

Subject headings: cosmology — galaxies: clustering — galaxies: formation

1. INTRODUCTION

The behavior of the distribution of galaxies on scales $\geq 10h^{-1}$ Mpc ($H_0 = 100h$ km s⁻¹ Mpc⁻¹) is a critical constraint on models for the formation of large-scale structure. Even the currently most popular cold dark matter model with biased galaxy formation (Davis *et al.* 1985) cannot produce voids as large as the one in Bootes discovered by Kirshner *et al.* (1981). In other words, if large voids are common, standard gravitational clustering models are unlikely to match the observations.

On the observational side there have been a number of discoveries of structures which extend for tens of Mpc. Zel'dovich, Einasto, and Shandarin (1982) emphasize a general cell-like structure in the galaxy distribution on these and larger scales. Two striking examples of individual large structures are the Perseus-Pisces chain (Gregory, Thompson, and Tift 1981), an apparently filamentary structure extending for $40h^{-1}$ Mpc, and the void in Bootes which has a volume of order $10^6 h^{-3}$ Mpc³. Taken at face value, the break in the correlation function at a scale of $15h^{-1}$ Mpc (Groth and Peebles 1977; Davis and Peebles 1983) indicates that structures as large as these must not be common. However, the determination of the behavior of the correlation function on large scales may be suspect because of biases in the galaxy catalogs (Geller, de Lapparent, and Kurtz 1984; de Lapparent, Kurtz, and Geller 1985).

This *Letter* is a preliminary discussion of recent results obtained as part of the extension of the Center for Astro-

physics redshift survey. Several features of the results are striking. The distribution of galaxies in the redshift survey slice looks like a slice through the suds in the kitchen sink; it appears that the galaxies are on the surfaces of bubble-like structures with diameter 25–50 h^{-1} Mpc. This topology poses serious challenges for current models for the formation of large-scale structure.

II. THE DATA

The sample is restricted to objects listed by Zwicky *et al.* (1961) with $m_B \leq 15.5$, $8^\circ \leq \alpha \leq 17^\circ$ and $26^\circ 5' \leq \delta \leq 32^\circ 5'$. On the sky, this survey covers a strip of $\sim 117^\circ \times 6^\circ$, centered near the north Galactic pole. We assigned magnitudes to the individual objects in multiple systems; galaxies are included in the sample only if they satisfy $m_B \leq 15.5$. The resulting catalog contains 1099 galaxies. Redshifts for the 186 galaxies brighter than $m_B = 14.5$ have been compiled by Huchra *et al.* in the CfA redshift survey (1982). Among the remaining redshifts, 327 have been published by other groups. The other 584 redshifts were measured with the Mount Hopkins 60 inch (1.5 m) telescope and the MMT, yielding a complete redshift survey. The data will be published elsewhere (Huchra *et al.* 1987).

Figure 1a shows a plot of the observed velocity versus right ascension for the galaxies brighter than $m_B = 15.5$ in the full 6° thick wedge; we only plot the 1061 objects with velocities less than 15,000 km s⁻¹. The effective depth of the sample is $\sim 100h^{-1}$ Mpc ($M^* = -19.4$; Davis and Huchra 1982). For contrast, we plot in Figure 1b the 182 objects with $m_B \leq 14.5$ and $V \leq 10,000$ km s⁻¹.

Figures 1a and 1b differ significantly in appearance. In Figure 1a, nearly every galaxy with $V \leq 10,000$ km s⁻¹ appears to be in a large structure. We argue below that the size of the largest of these bubble-like structures is comparable



JOHN HUCHRA

DE LAPPARENT, GELLER, AND HUCHRA

Vol. 302

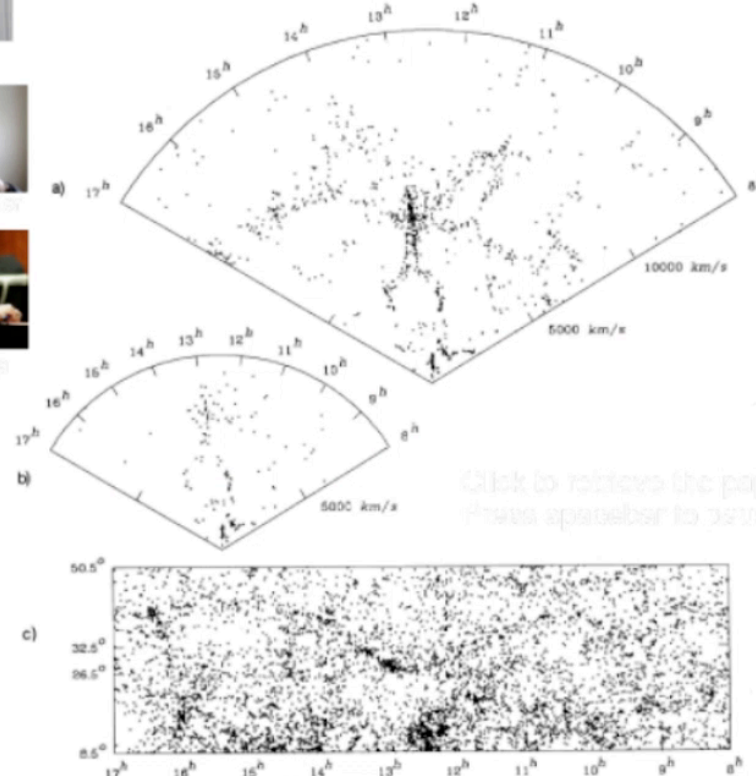


FIG. 1.—(a) Map of the observed velocity plotted vs. right ascension in the declination wedge $26^\circ 5' \leq \delta \leq 32^\circ 5'$. The 1061 objects plotted have $m_B \leq 15.5$ and $V \leq 15,000$ km s⁻¹. (b) Same as Fig. 1a for $m_B \leq 14.5$ and $V \leq 10,000$ km s⁻¹. The plot contains 182 galaxies. (c) Projected map of the 7031 objects with $m_B \leq 15.5$, binned by Zwicky *et al.* in the region bounded by $8^\circ \leq \alpha \leq 17^\circ$ and $8^\circ 5' \leq \delta \leq 50^\circ 5'$.

with the depth of the earlier survey. Thus undersampling explains the difference in the appearance of the surveys.

In order to compare the redshift-space distribution with the distribution projected on the sky, Figure 1c shows the positions of all the galaxies from the Zwicky *et al.* catalog which satisfy $m_B \leq 15.5$, $8^\circ \leq \alpha \leq 17^\circ$ and $8^\circ 5' \leq \delta \leq 50^\circ 5'$. The grid is Cartesian in R.A. and decl. The deficiency of galaxies west of 9° and east of 16° is caused by Galactic obscuration. The tick marks show the 6° declination region of the redshift survey in Figure 1a. The Coma cluster is the dense region at 13° in the 6° strip.

III. ANALYSIS

The cellular pattern of Figure 1a and the smoothness of Figure 1c can be simply understood if the galaxies are distributed on the surfaces of shells tightly packed next to each other. If shell-like structures are common in the universe, any sufficiently deep wedge-shaped redshift survey will show a pattern of voids surrounded by connected filaments of galaxies similar to that in Figure 1a.

One impressive feature of the new data in Figure 1a is the presence of several large regions almost devoid of galaxies. The galaxies appear to be distributed in elongated structures

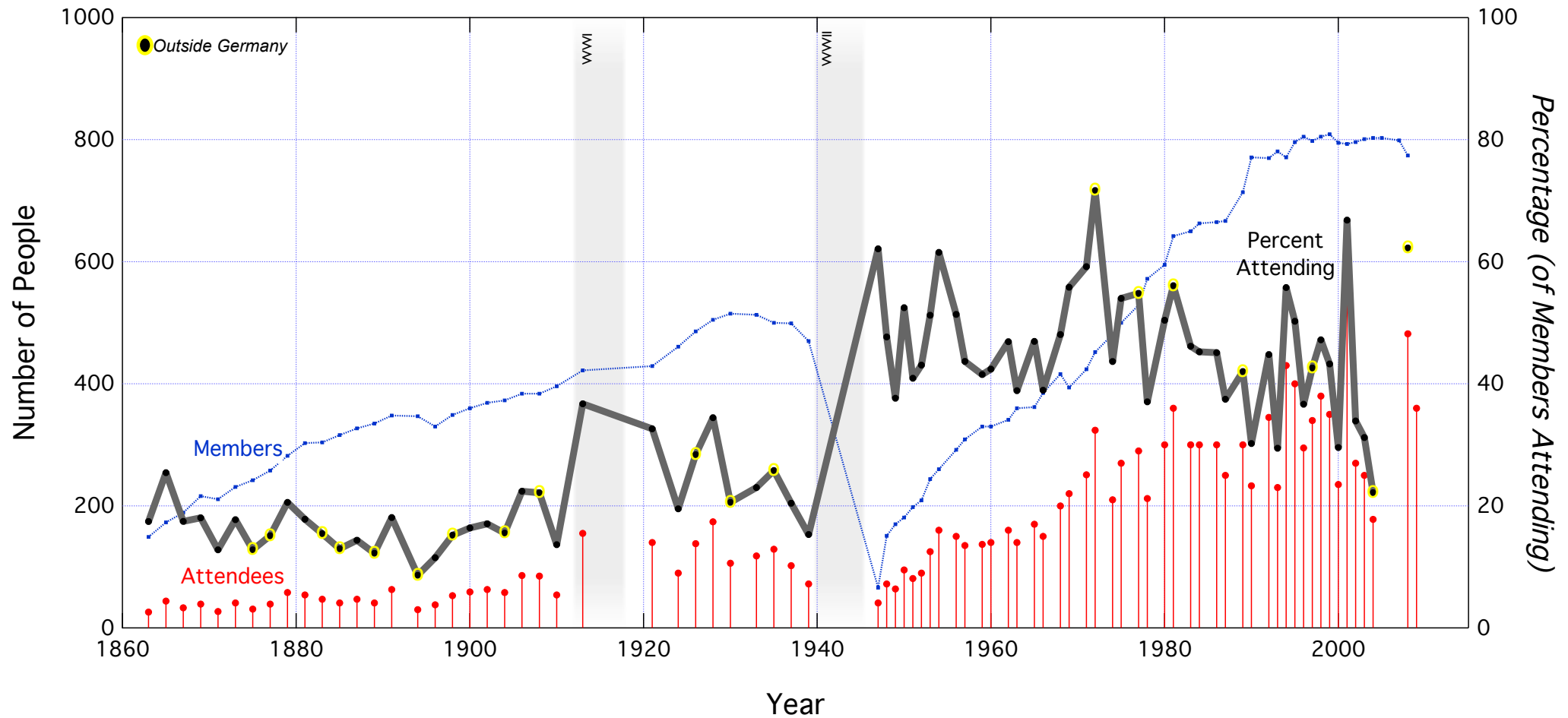
¹ Based partly on results obtained with the Multiple Mirror Telescope, a facility operated jointly by the Smithsonian Institution and the University of Arizona.

² Harvard-Smithsonian Center for Astrophysics.

³ Ecole Normale Supérieure de Jeunes Filles and Université Paris VII, Paris.

"HIGH-DIMENSIONAL"

need not mean spatial
need not be displayed in >2D



example from Goodman 2012: "Principles of High-Dimensional Data Visualization in Astronomy"

"HIGH-DIMENSIONAL"

need not mean spatial
need not be displayed in >2D

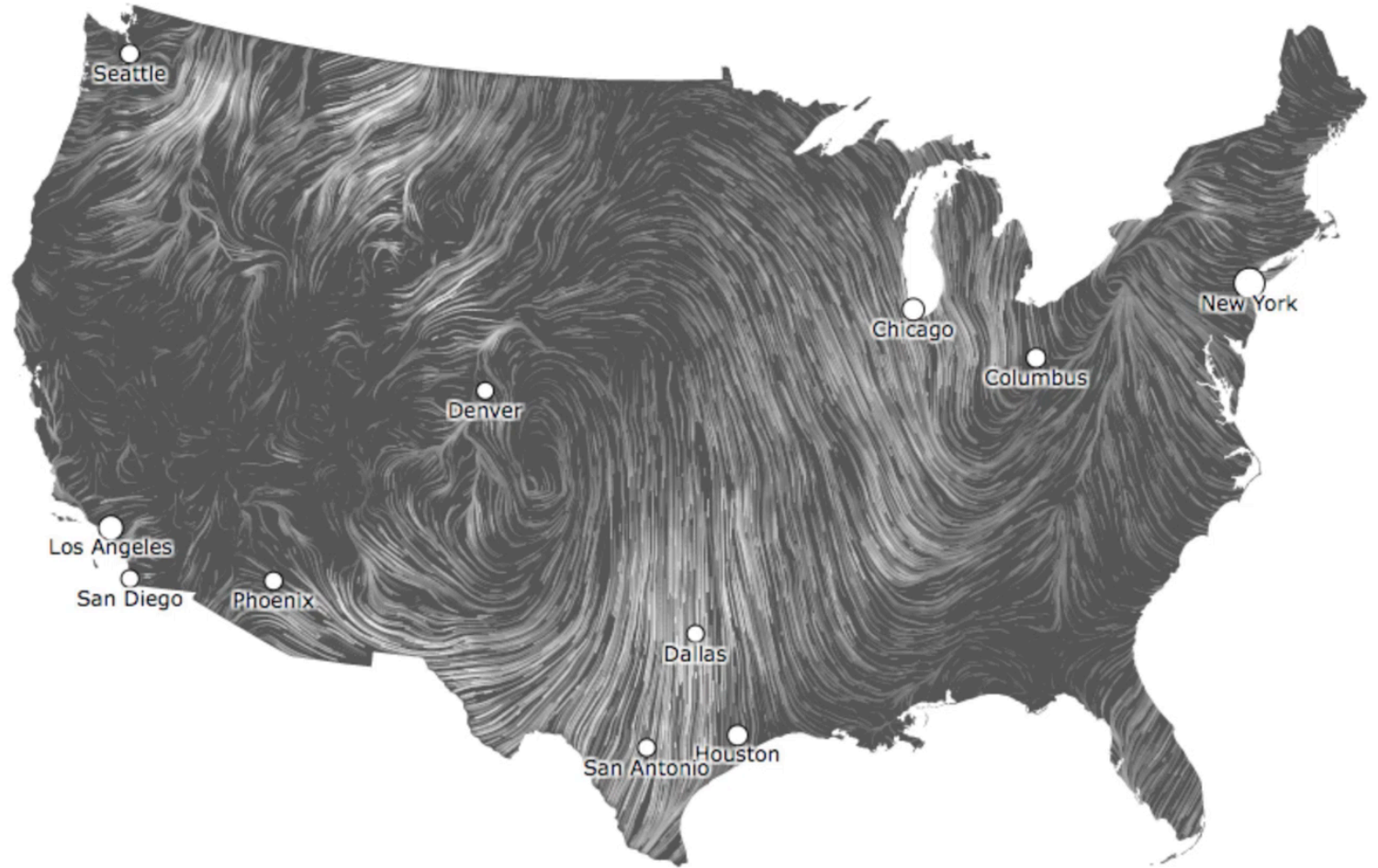
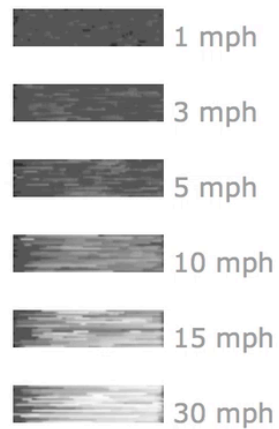
wind map

October 20, 2016

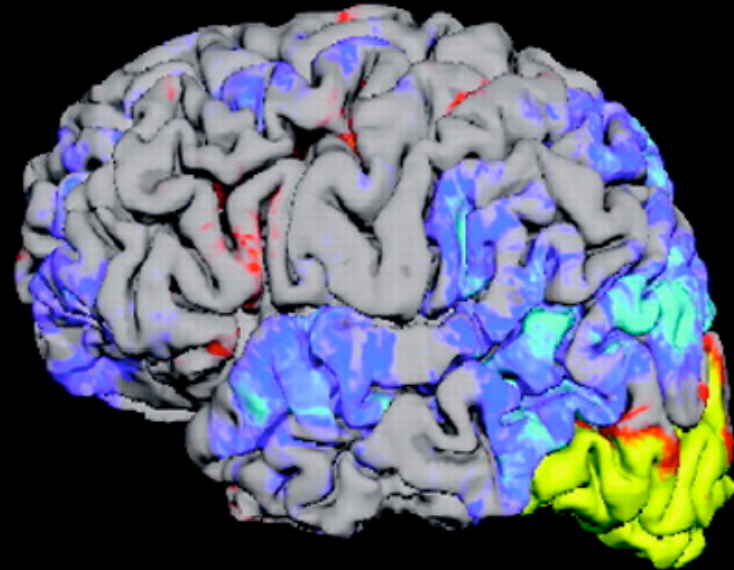
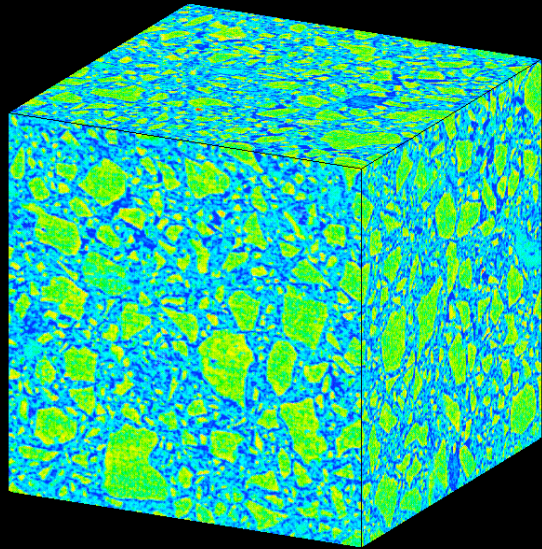
4:35 pm EST

(time of forecast download)

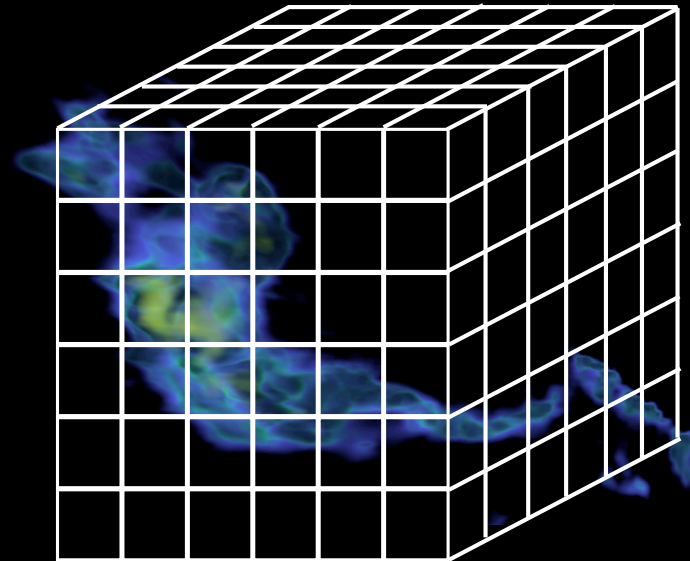
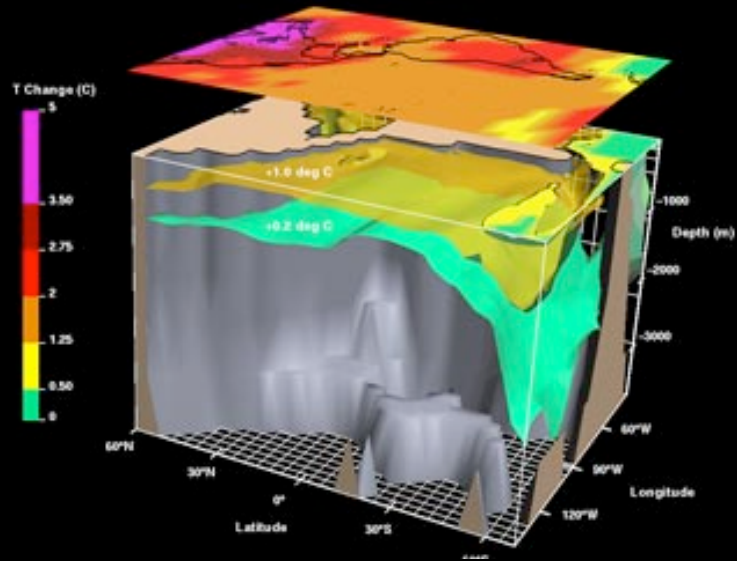
top speed: **33.2 mph**
average: **8.5 mph**

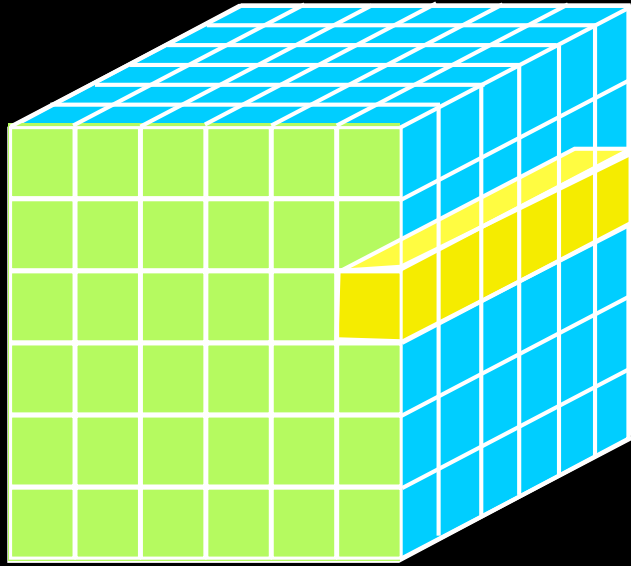


"HIGH-DIMENSIONAL" DATA



ATMOSPHERIC AND OCEANIC TEMPERATURE CHANGE





DATA-DIMENSIONS-DISPLAY

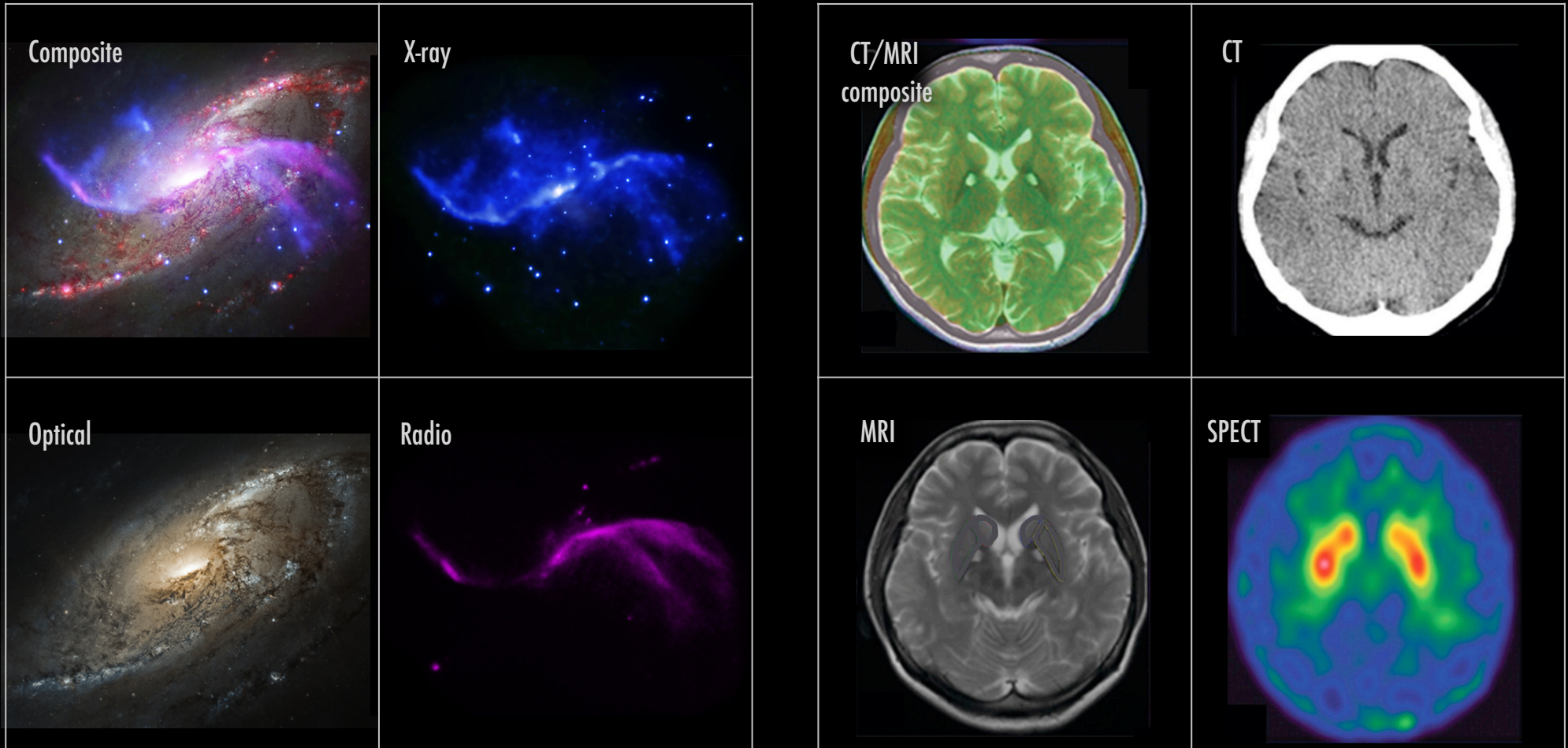
1D: Columns = "Spectra", "SEDs" or "Time Series" (x-y Graphs)

2D: Faces or Slices = "Images"

3D: Volumes = "3D Renderings", "2D Movies"

4D: Time Series of Volumes = "3D Movies"

ASTRONOMICAL MEDICINE

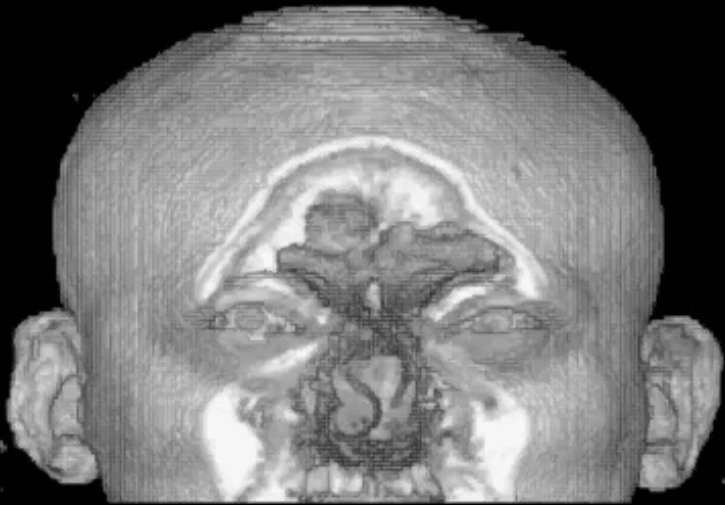


chandra.harvard.edu/photo/2014/m106/

Chang, et al. 2011, brain.oxfordjournals.org/content/134/12/3632

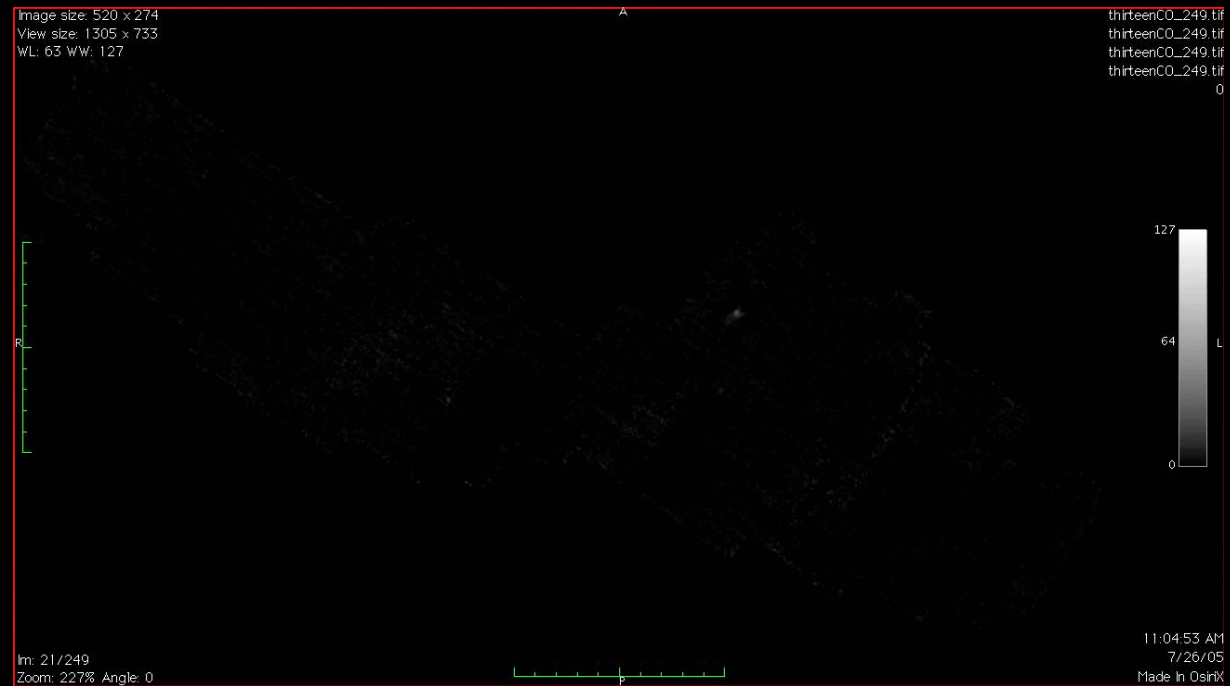
ASTRONOMICAL MEDICINE

"KEITH"



"z" is depth into head

"PERSEUS"

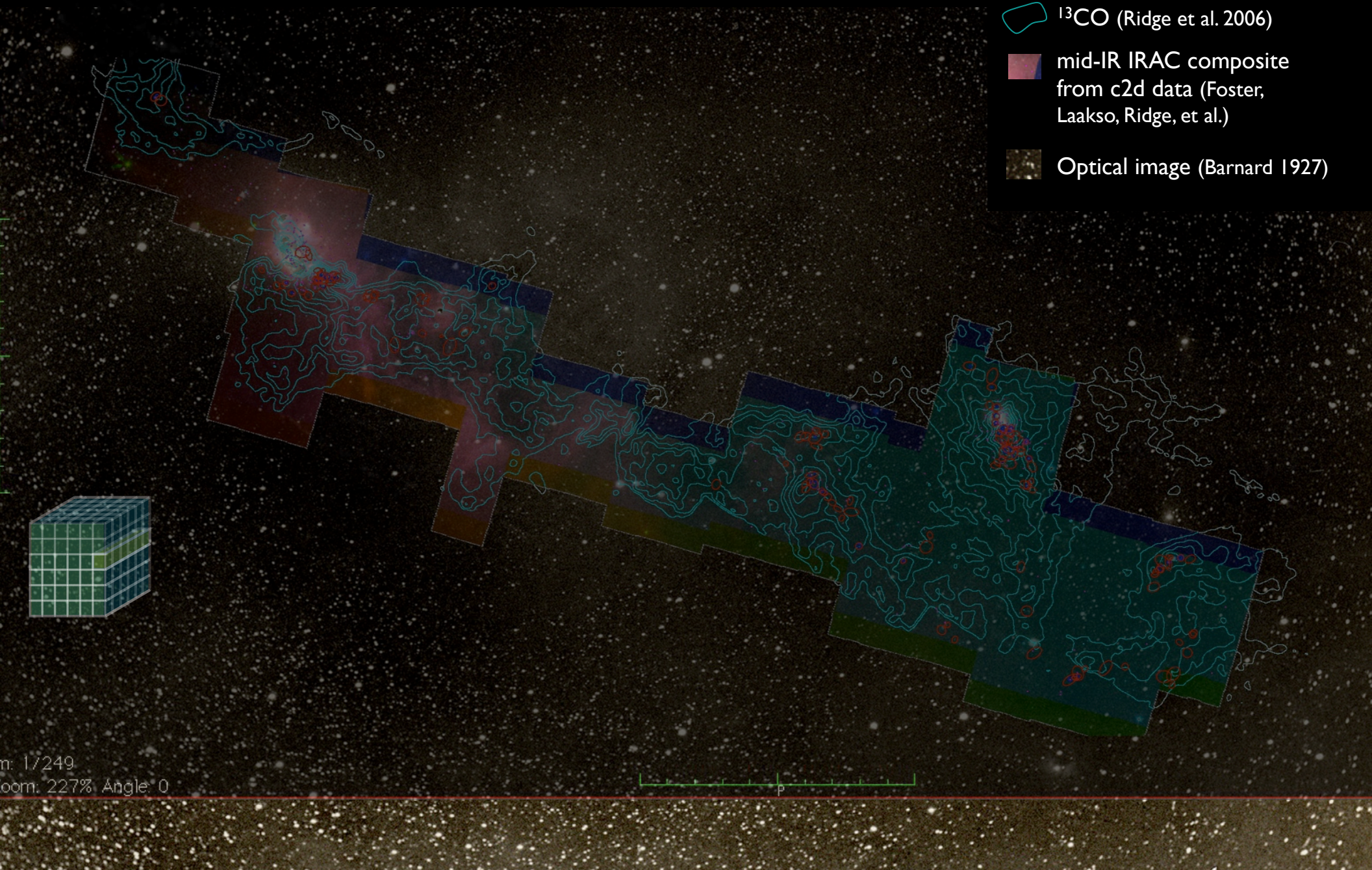


"z" is line-of-sight velocity

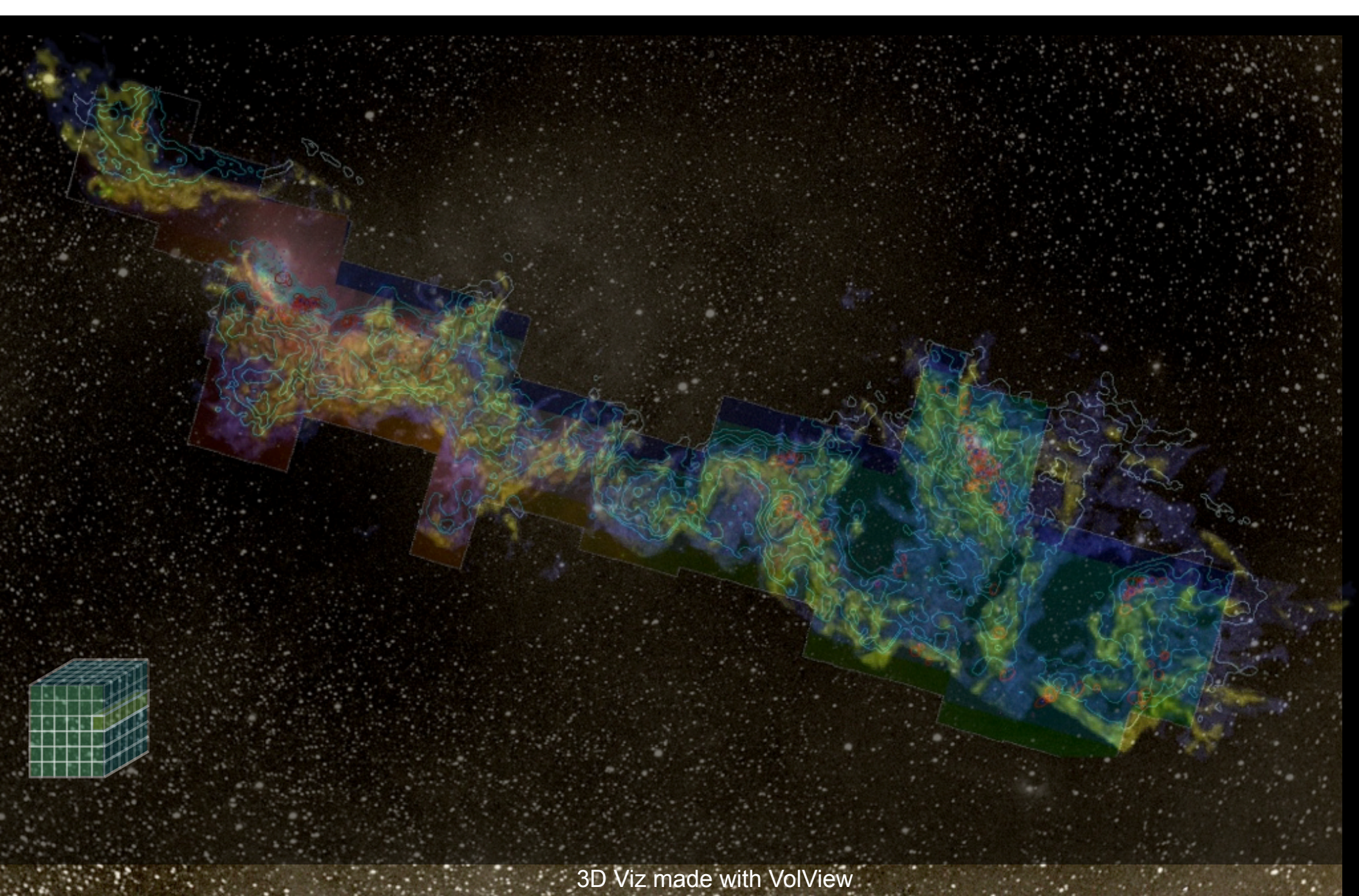
Image size: 520 x 274
View size: 1305 x 733
W/L: 63 WW: 127

ASTRONOMICAL MEDICINE

-  mm peak (Enoch et al. 2006)
-  sub-mm peak (Hatchell et al. 2005, Kirk et al. 2006)
-  ^{13}CO (Ridge et al. 2006)
-  mid-IR IRAC composite from c2d data (Foster, Laakso, Ridge, et al.)
-  Optical image (Barnard 1927)



m: 1/249
Zoom: 227% Angle: 0



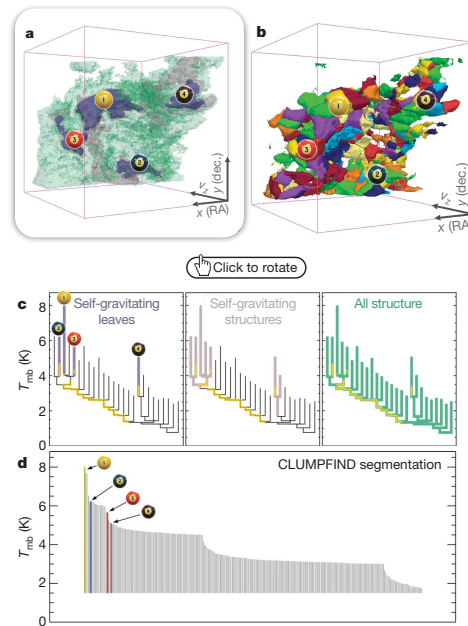


Figure 2 | Comparison of the 'dendrogram' and 'CLUMPFIND' feature-identification algorithms as applied to ^{13}CO emission from the L1448 region of Perseus. **a**, 3D visualization of the surfaces indicated by colours in the dendrogram shown in **c**. Purple illustrates the smallest scale self-gravitating structures in the region corresponding to the leaves of the dendrogram; pink shows the smallest surfaces that contain distinct self-gravitating leaves within them; and green corresponds to the surface in the data cube containing all the significant emission. Dendrogram branches corresponding to self-gravitating objects have been highlighted in yellow over the range of T_{mb} (main-beam temperature) test-level values for which the virial parameter is less than 2. The x - y locations of the four 'self-gravitating' leaves labelled with billiard balls are the same as those shown in Fig. 1. The 3D visualizations show position–position–velocity (p - p - v) space. RA, right ascension; dec., declination. For comparison with the ability of dendrograms (**c**) to track hierarchical structure, **d** shows a pseudo-dendrogram of the CLUMPFIND segmentation (**b**), with the same four labels used in Fig. 1 and in **a**. As 'clumps' are not allowed to belong to larger structures, each pseudo-branch in **d** is simply a series of lines connecting the maximum emission value in each clump to the threshold value. A very large number of clumps appears in **b** because of the sensitivity of CLUMPFIND to noise and small-scale structure in the data. In the online PDF version, the 3D cubes (**a** and **b**) can be rotated to any orientation, and surfaces can be turned on and off (interaction requires Adobe Acrobat version 7.0.8 or higher). In the printed version, the front face of each 3D cube (the 'home' view in the interactive online version) corresponds exactly to the patch of sky shown in Fig. 1, and velocity with respect to the Local Standard of Rest increases from front (-0.5 km s^{-1}) to back (8 km s^{-1}).

data, CLUMPFIND typically finds features on a limited range of scales, above but close to the physical resolution of the data, and its results can be overly dependent on input parameters. By tuning CLUMPFIND's two free parameters, the same molecular-line data set⁸ can be used to show either that the frequency distribution of clump mass is the same as the initial mass function of stars or that it follows the much shallower mass function associated with large-scale molecular clouds (Supplementary Fig. 1).

Four years before the advent of CLUMPFIND, 'structure trees'⁹ were proposed as a way to characterize clouds' hierarchical structure

using 2D maps of column density. With the help of 2D work as inspiration, we have developed a structure-identification algorithm that abstracts the hierarchical structure of a data set into an easily visualized representation called a dendrogram. This method, well developed in other data-intensive fields, has been applied to the application of tree methodologies so far, and almost exclusively within the area of astronomy. Dendrograms and 'merger trees' are being used with increasing frequency.

Figure 3 and its legend explain the dendrogram process schematically. The dendrogram quantifies the hierarchy of emission merge with each other. The dendrogram is explained in Supplementary Methods and Supplementary Fig. 1. It is determined almost entirely by the sensitivity to algorithm parameters, which can be varied as possible on paper and 2D screen data (see Fig. 3 and its legend). The dendrogram is a sorted dendrogram, which eliminates dimensions, preserving all information. Numbered 'billiard ball' labels are used to identify key features between a 2D map and a sorted dendrogram (see Fig. 3 and its legend).

A dendrogram of a spectrum of key physical properties, such as radius (R), mass (M), luminosity (L), and virial parameter (α). The volumes can have any shape, and the significance of the especially elongated features is quantified (Fig. 2a). The luminosity is an approximate proxy for mass, such that $M_{\text{lum}} = X_{13\text{CO}} L_{13\text{CO}}$, where $X_{13\text{CO}} = 8.0 \times 10^{20} \text{ cm}^{-2} \text{ K}^{-1} \text{ km}^{-1} \text{ s}$ (ref. 15; see Supplementary Methods and Supplementary Fig. 2). The derived values for size, mass and velocity dispersion can then be used to estimate the role of self-gravity at each point in the hierarchy, via calculation of an 'observed' virial parameter, $\alpha_{\text{obs}} = 5\sigma_v^2 R/GM_{\text{lum}}$. In principle, extended portions of the tree (Fig. 2, yellow highlighting) where $\alpha_{\text{obs}} < 2$ (where gravitational energy is comparable to or larger than kinetic energy) correspond to regions of p - p - v space where self-gravity is significant. As α_{obs} only represents the ratio of kinetic energy to gravitational energy at one point in time, and does not explicitly capture external over-pressure and/or magnetic fields¹⁶, its measured value should only be used as a guide to the longevity (boundedness) of any particular feature.

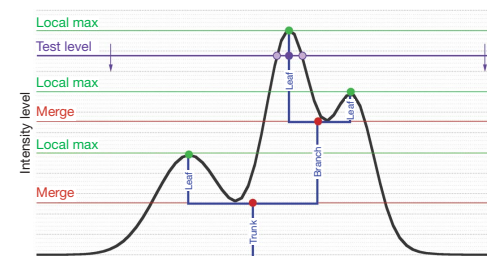
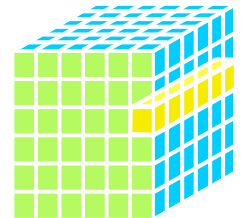
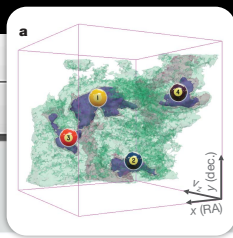


Figure 3 | Schematic illustration of the dendrogram process. Shown is the construction of a dendrogram from a hypothetical one-dimensional emission profile (black). The dendrogram (blue) can be constructed by 'dropping' a test constant emission level (purple) from above in tiny steps (exaggerated in size here, light lines) until all the local maxima and mergers are found, and connected as shown. The intersection of a test level with the emission is a set of points (for example the light purple dots) in one dimension, a planar curve in two dimensions, and an isosurface in three dimensions. The dendrogram of 3D data shown in Fig. 2c is the direct analogue of the tree shown here, only constructed from 'isosurface' rather than 'point' intersections. It has been sorted and flattened for representation on a flat page, as fully representing dendrograms for 3D data cubes would require four dimensions.

2009
3D PDF
HIGH-DIMENSIONAL
DATA IN A
"PAPER"



Goodman et al. 2009, Nature,
cf: Fluke et al. 2009



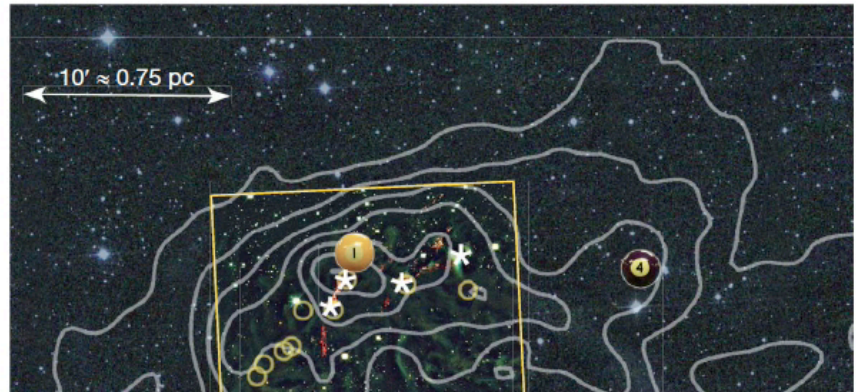
LETTERS

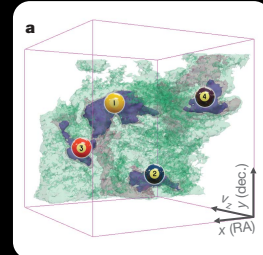
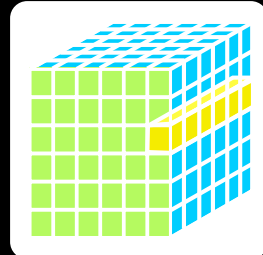
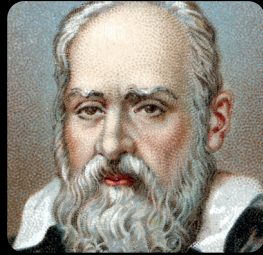
A role for self-gravity at multiple length scales in the process of star formation

Alyssa A. Goodman^{1,2}, Erik W. Rosolowsky^{2,3}, Michelle A. Borkin^{1†}, Jonathan B. Foster², Michael Halle^{1,4}, Jens Kauffmann^{1,2} & Jaime E. Pineda²

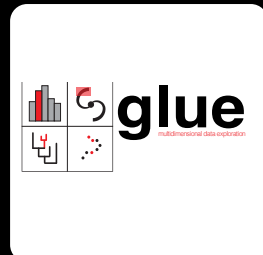
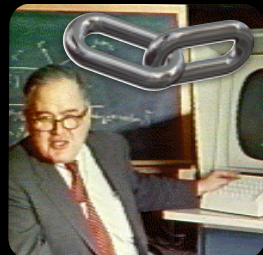
Self-gravity plays a decisive role in the final stages of star formation, where dense cores (size ~ 0.1 parsecs) inside molecular clouds collapse to form star-plus-disk systems¹. But self-gravity's role at earlier times (and on larger length scales, such as ~ 1 parsec) is unclear; some molecular cloud simulations that do not include self-gravity suggest that 'turbulent fragmentation' alone is sufficient to create a mass distribution of dense cores that resembles, and sets, the stellar initial mass function². Here we report a 'denrogram' (hierarchical tree-diagram) analysis that reveals that self-gravity plays a significant role over the full range of possible scales traced by ¹³CO observations in the L1448 molecular cloud, but not everywhere in the observed region. In particular, more than 90 per cent of the compact 'pre-stellar cores' traced by peaks of dust emission³ are projected on the sky within one of the denrogram's self-gravitating 'leaves'. As these peaks mark the locations of already-forming stars, or of those probably about to form, a self-gravitating cocoon seems a critical condition for their exist-

overlapping features as an option, significant emission found between prominent clumps is typically either appended to the nearest clump or turned into a small, usually 'pathological', feature needed to encompass all the emission being modelled. When applied to molecular-line





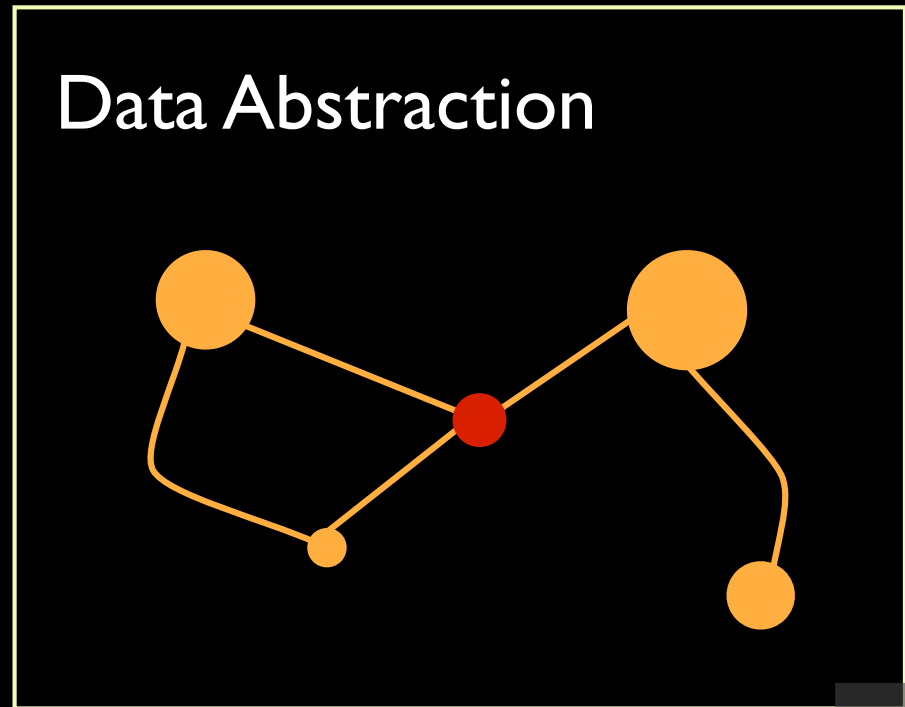
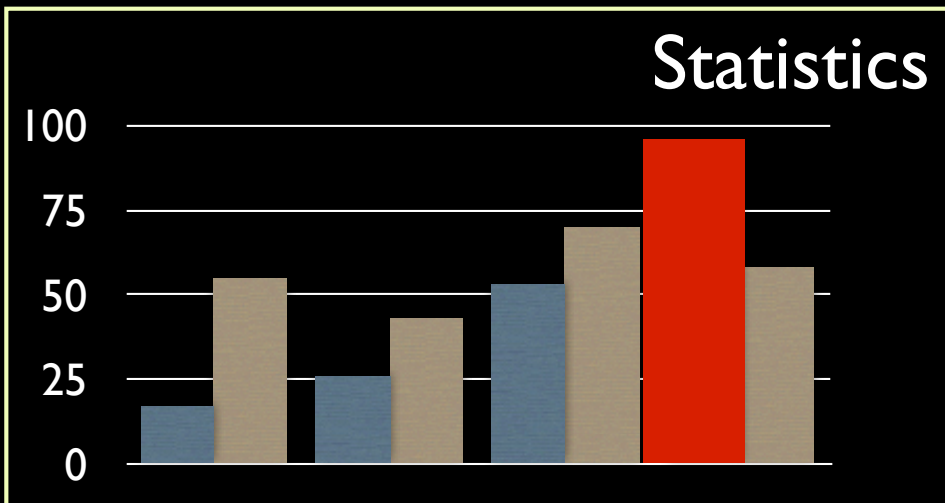
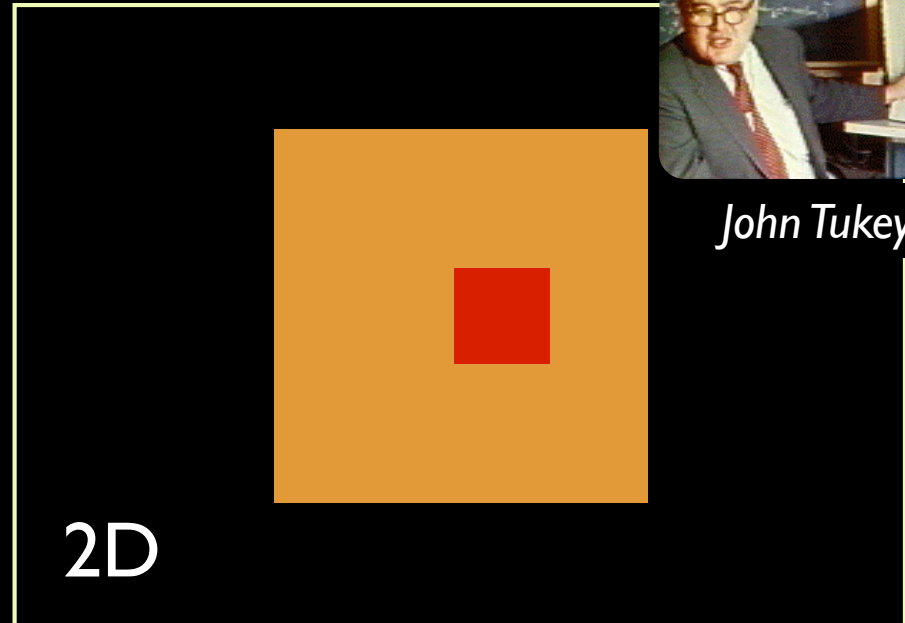
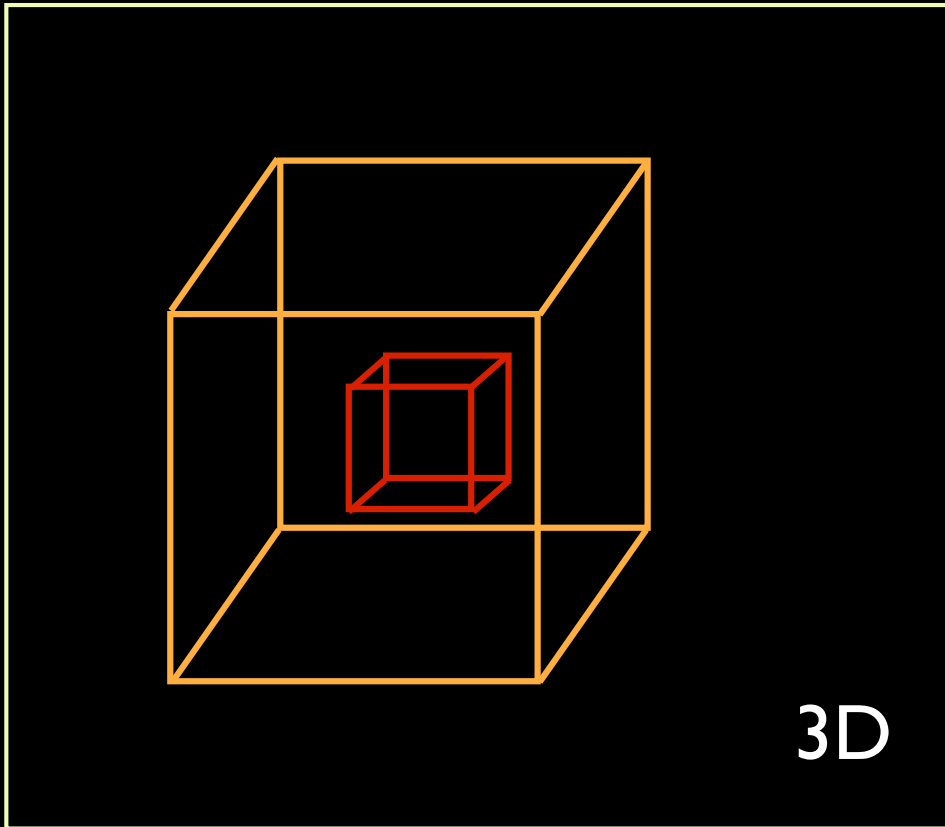
So, by 2009 we could “publish” what Galileo had in mind.
Today, though, we want to **explore** big, wide, data sets, live.



LINKED VIEWS OF HIGH-DIMENSIONAL DATA

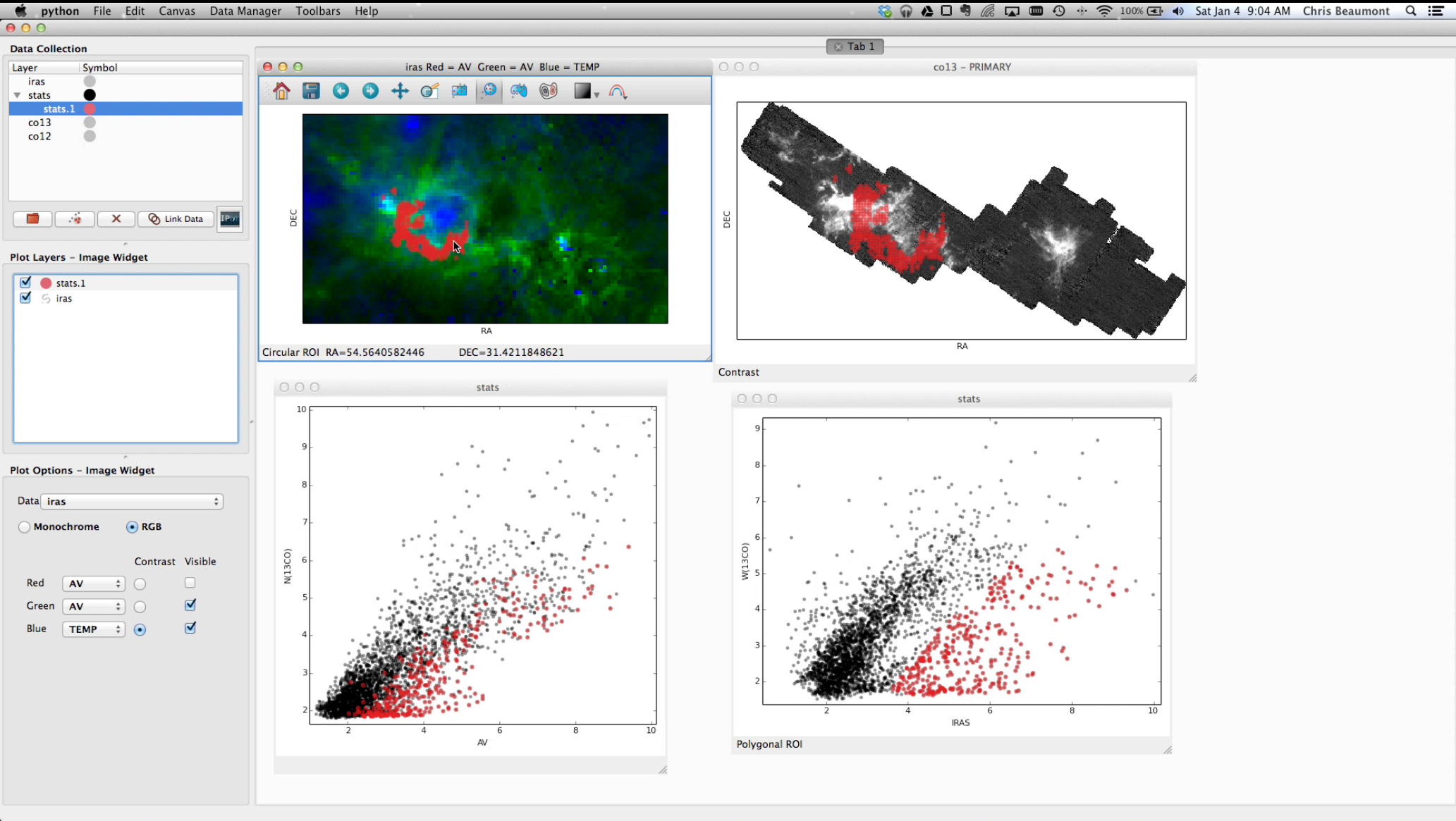
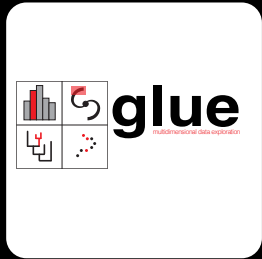


John Tukey



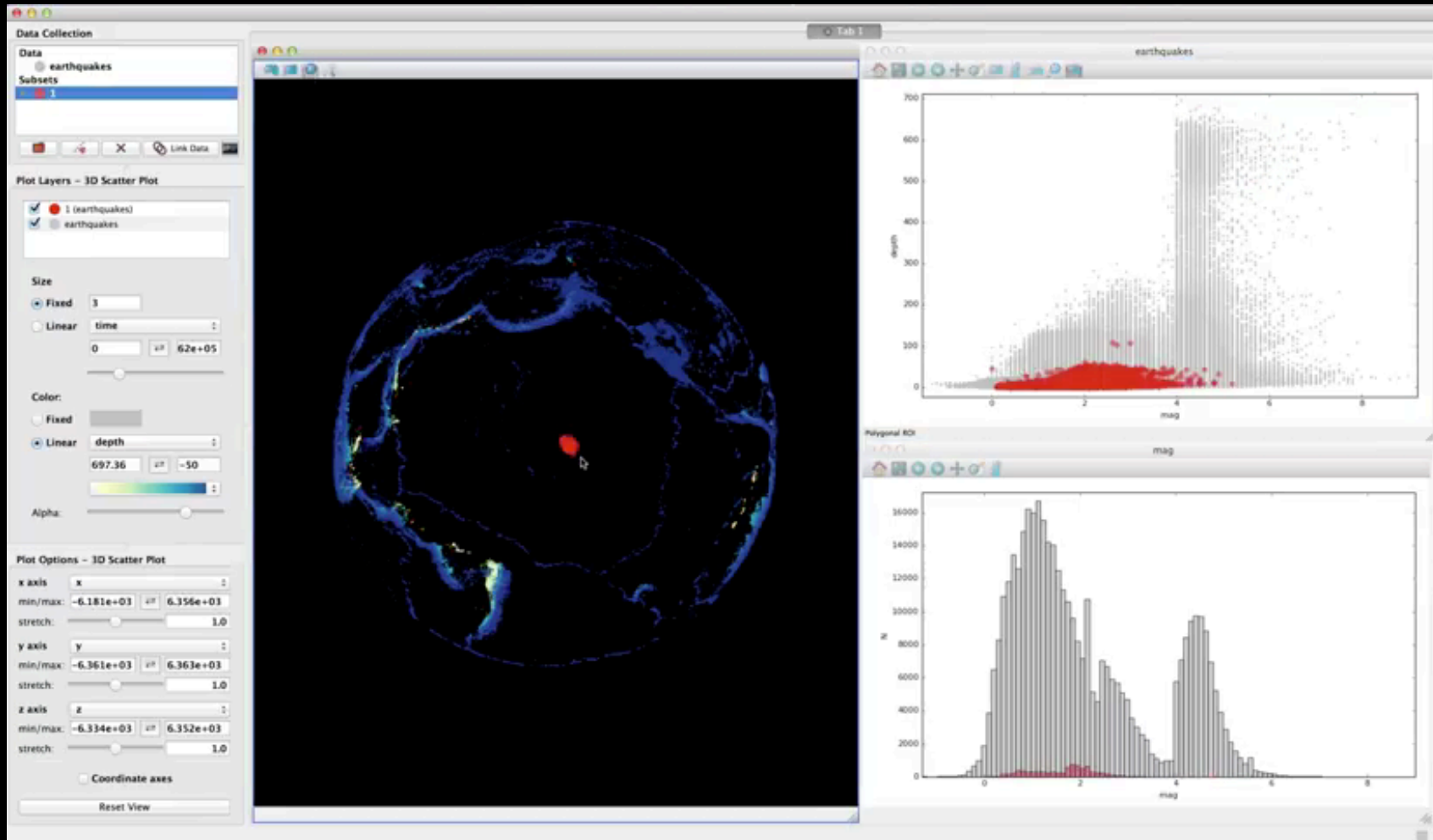
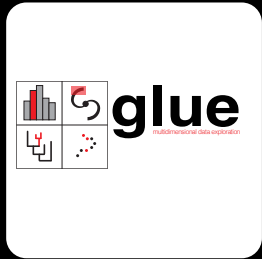
LINKED VIEWS OF HIGH-DIMENSIONAL DATA (IN PYTHON)

GLUE



LINKED VIEWS OF HIGH-DIMENSIONAL DATA (IN PYTHON)

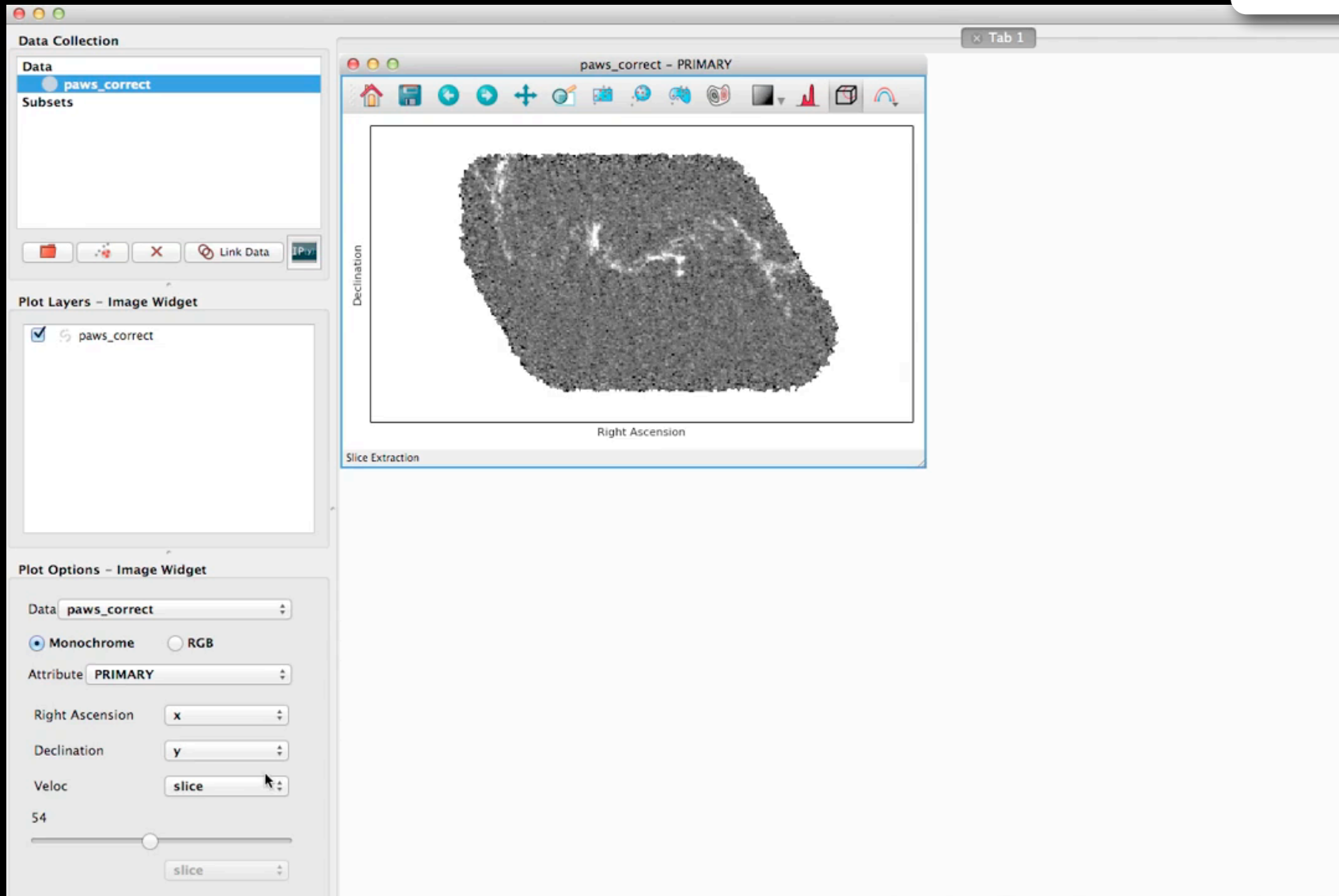
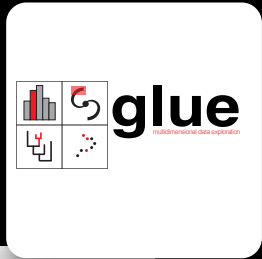
GLUE



*video by Tom Robitaille, lead glue developer
glue created by: C. Beaumont, M. Borkin, P. Qian, T. Robitaille, and A. Goodman, PI*

LINKED VIEWS OF HIGH-DIMENSIONAL DATA (IN PYTHON)

GLUE



*video by Chris Beaumont, glue developer
glue created by: C. Beaumont, M. Borkin, P. Qian, T. Robitaille, and A. Goodman, PI*



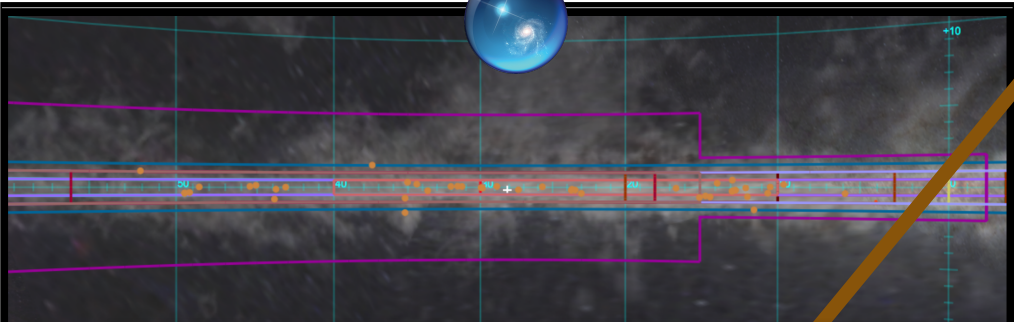
[+demo]

WIDE, BIG, OPEN DATA

 **Milky Way 3D**
Galactic Plane Coverage Tool

milkyway3d.org

MilkyWay3D.org is a tool intended to organize and curate links to information about data sets relevant to our 3D understanding of the Milky Way. For any given longitude range, we provide the means to determine the available surveys, their overlapping footprint, and the type of data each provides. Information about each dataset, including how to access the data, their hallmark publications, and their principal investigators, is available at the [Milky Way 3D Dataverse](#). All the data can be loaded, "linked", and explored using the new 3D visualization software package Glue, available for download at [glueviz.org](#)!



This is an interactive... of a region, click on... the data in the region

View Region	Link to Survey	Wavelength	Extended Observations		Catalogs and Pointed Surveys	
			Continuum (2D)	Spectral Line (3D)	Source-Based Lists	Spectral Line
<input checked="" type="checkbox"/>	THOR	21 cm, 300 mm, 174-186 mm		★		
<input checked="" type="checkbox"/>	BESSEL	1-3 cm			★	
<input checked="" type="checkbox"/>	RAMPS*	1 cm		★		
<input checked="" type="checkbox"/>	CORNISH*	60 mm	★		★	
<input checked="" type="checkbox"/>	HOPS	12 mm		★		★
<input checked="" type="checkbox"/>	GRS	3 mm		★		
<input checked="" type="checkbox"/>	MALT90	3 mm				★
<input checked="" type="checkbox"/>	THRUMMS	3 mm		★		
<input checked="" type="checkbox"/>	Dame CO	2.6 mm		★		
<input checked="" type="checkbox"/>	BGPS	1 mm	★		★	★
<input checked="" type="checkbox"/>	CHIMPS	1 mm		★		
<input checked="" type="checkbox"/>	COHRS	1 mm		★		
<input checked="" type="checkbox"/>	ATLASGAL	870 μm	★		★	
<input checked="" type="checkbox"/>	JCMT*	850 μm	★		★	
<input checked="" type="checkbox"/>	HIGAL*	70-500 μm	★			
<input checked="" type="checkbox"/>	MIPSGAL	24, 70 μm	★			
<input checked="" type="checkbox"/>	WISE	3.4, 4.6, 12, 22.0 μm	★			
<input checked="" type="checkbox"/>	GLIMPSE	3.6, 4.5, 5.8, 8.0 μm	★			

Admin ▼ |  Alyssa Ann Goodman ▼

 **VIALACTEA Science Gateway**

- Welcome ▼
- Workflow ▼
- Storage ▼
- Settings ▼
- Security ▼
- Statistics
- Information ▼
- Data Avenue
- Help ▼
- End User ▼
- PBS Monitoring ▼

Data Avenue

DataAvenue

and coming soon!

Two panel view
Edit favorites
History

Powered By [Liferay](#)

Subject
[Astronomy and Astrophysics \(1\)](#)

Author Name
[Simon Bihl \(1\)](#)

are a variety of data products available. The first includes HI 21 cm observations with a bandwidth of 2 MHz and a channel width of 1.953 kHz. Thi...

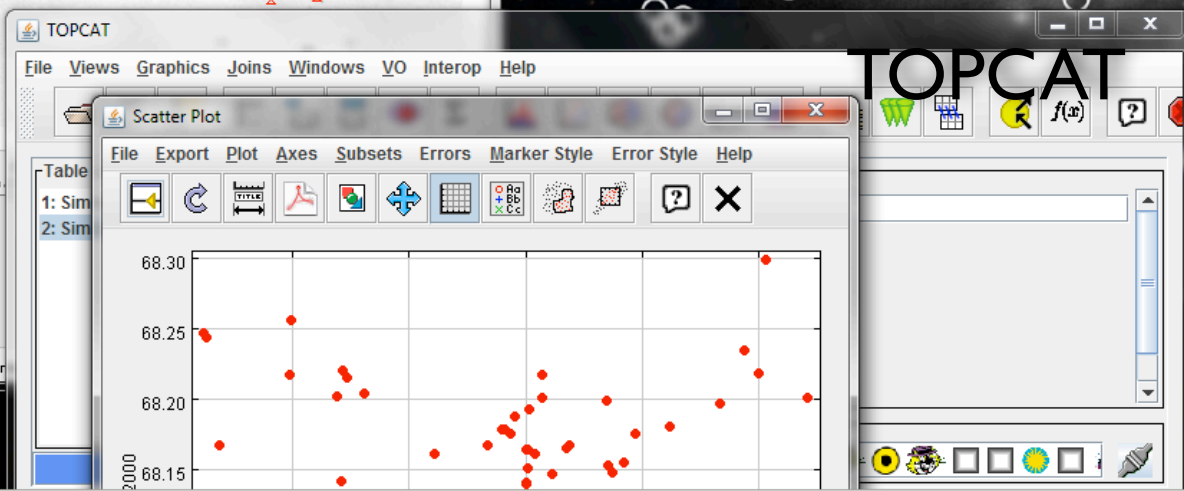
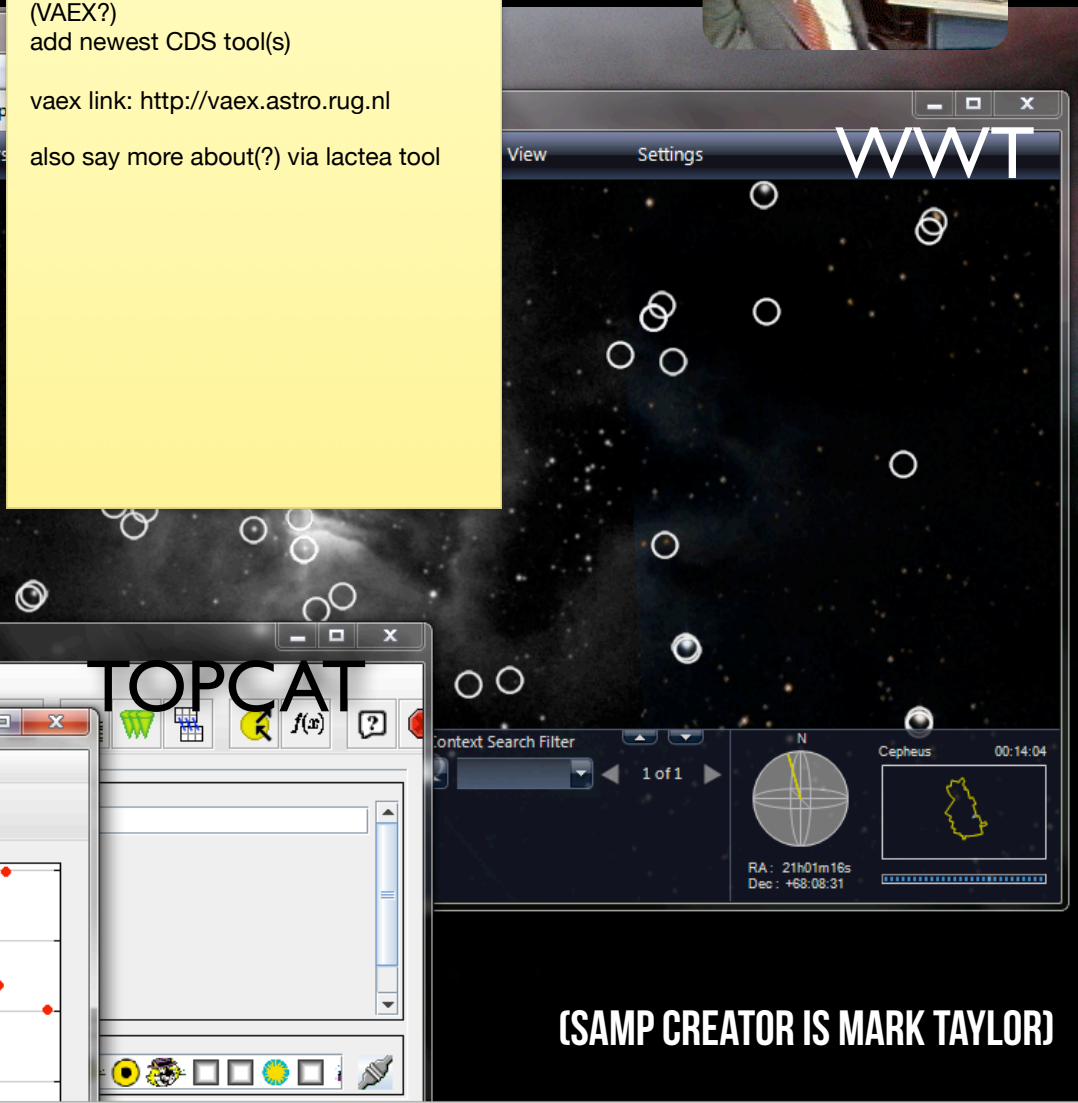
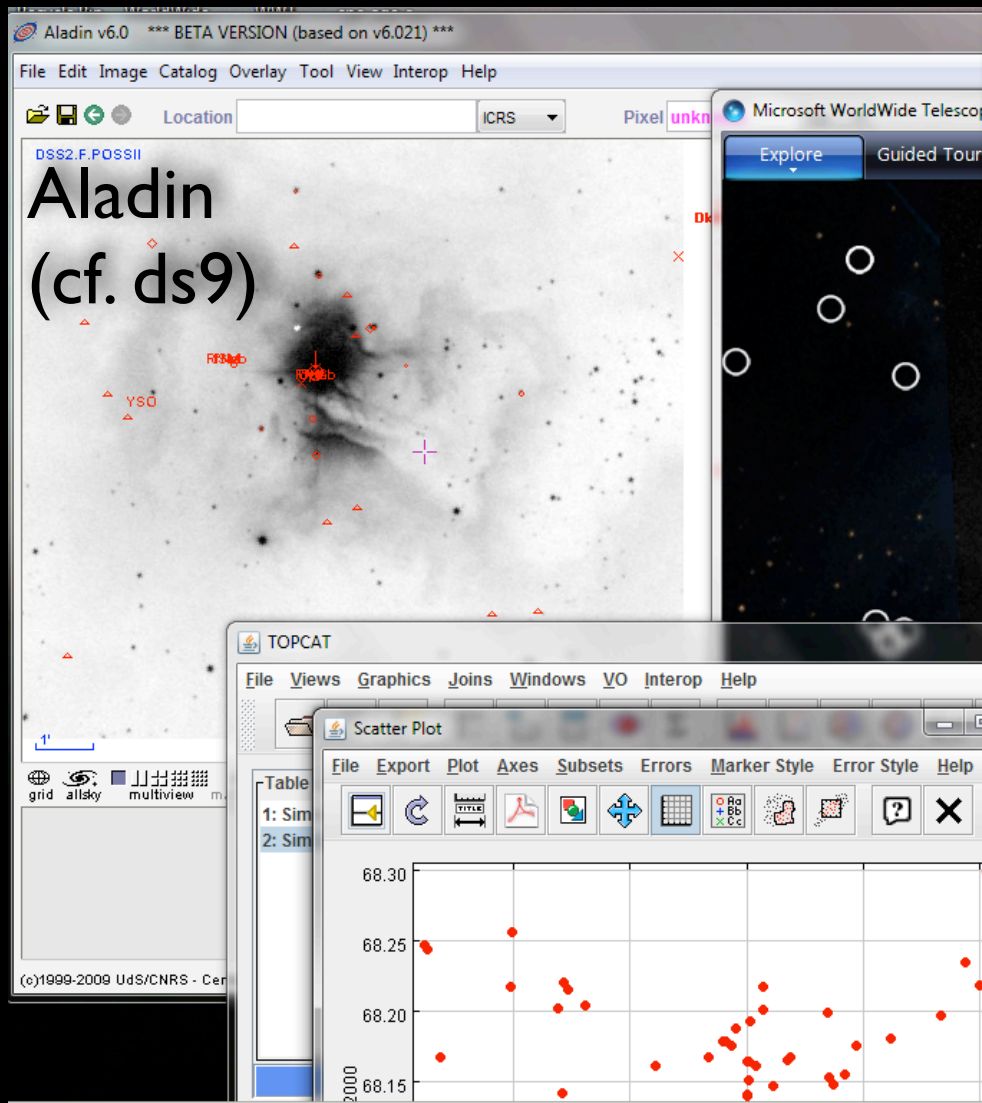
LINKED VIEWS OF HIGH-DIMENSIONAL DATA "SAMP"



update this slide re:TOPCAT, SAMP,
(VAEX?)
add newest CDS tool(s)

vaex link: <http://vaex.astro.rug.nl>

also say more about(?) via lactea tool



(SAMP CREATOR IS MARK TAYLOR)

figure, showing SAMP screenshot, reproduced from Goodman 2012, "Principles of High-Dimensional Data Visualization in Astronomy"

ADDING METADATA "DIMENSIONS"

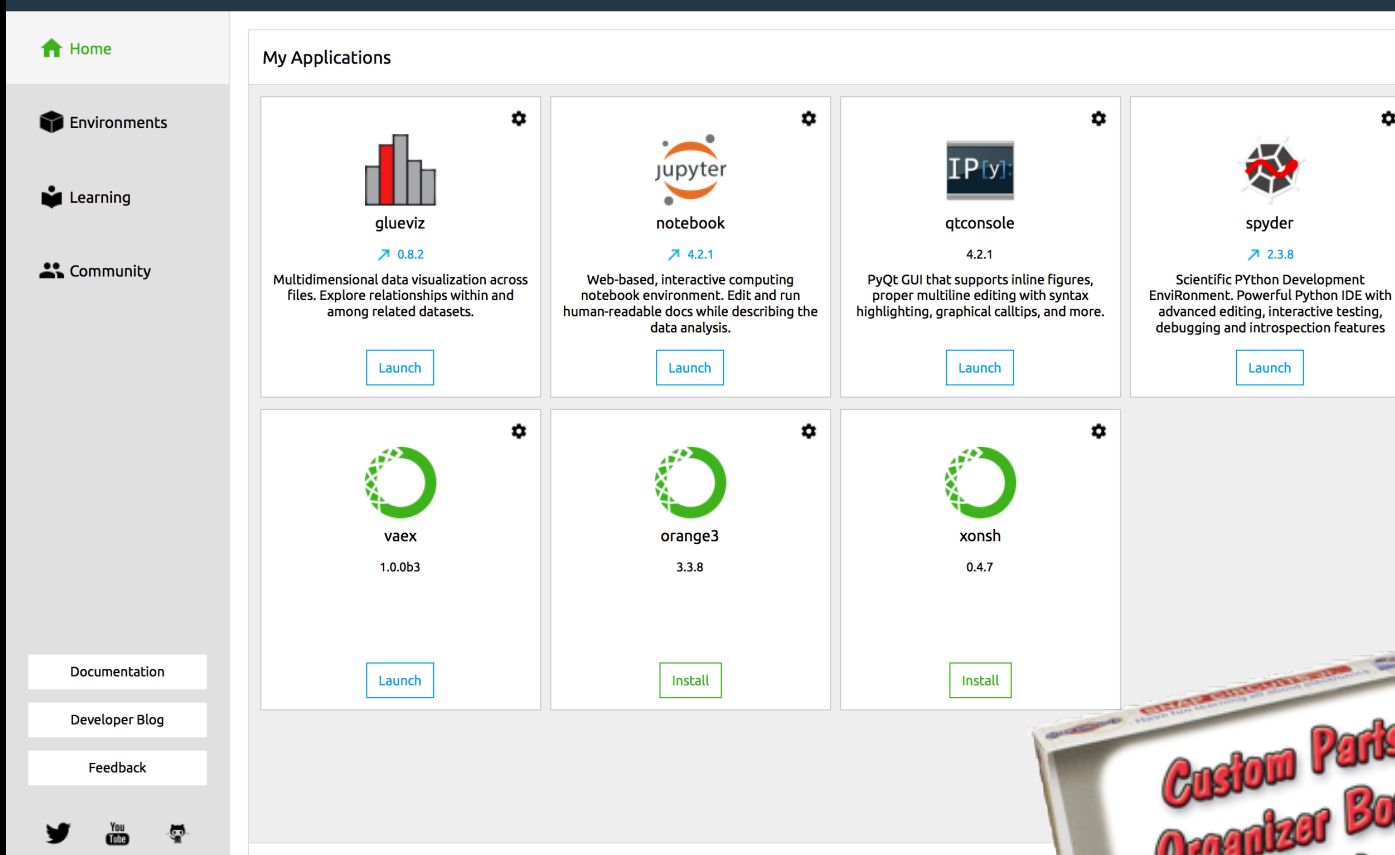
The screenshot shows the ADS All-Sky Survey web interface. The browser address bar displays the URL: www.adsass.org/wwt/?ra=345.42886923995724&dec=56.80696913940664&fov=118.07887634625072&layer=harvard. The page header includes "The ADS All Sky Survey" and "Open Aladin version".

The main content area features a star field heatmap. On the left, there are control panels:

- CHOOSE HEATMAP:** Includes buttons for "Object" (All Stars, Galaxies, HII regions, Nebulae, Other), "Band" (Radio, Infrared, Ultraviolet, X-ray), "Custom" (Harvard/All), and "Year" (slider).
- BACKGROUND LAYER:** Includes buttons for "Optical" (2MASS, WISE, SFD, IRIS, GLIMPSE, H-alpha, ROSAT) and "Optical" (Harvard/All).

A "Show Sources" button and a "Go to..." search box are also present. A large blue circular logo with a red swoosh and the text "ADS ALL SKY SURVEY" is overlaid on the heatmap. At the bottom left, a status bar shows: $(\alpha, \delta) = 83.66^\circ, -5.39^\circ$ FOV = 17° . At the bottom center, a footer states: "ADS All-Sky Survey is a NASA-funded project".

THE FUTURE IS ABOUT INTEGRATION



THE FUTURE IS ABOUT INTEGRATION



Explore Guided Tours Search Communities View Settings Install Windows Client

Collections > All-Sky Surveys >

Up Level More Surveys Digitized Sky VLSS: VLA Low- WMAP ILC 5-Year Planck CMB Planck Dust & Gas SFD Dust Map IRIS: Improved WISE All Sky

Look At Sky Imagery SFD Dust Map (Infrared)

Uranus MACS J0025.4-1222 Arp 256 NGC 17, NGC 34* IC 1623A/B



CDS Portal Simbad Vizier Aladin X-Match Other Help

HiPS list aggregator

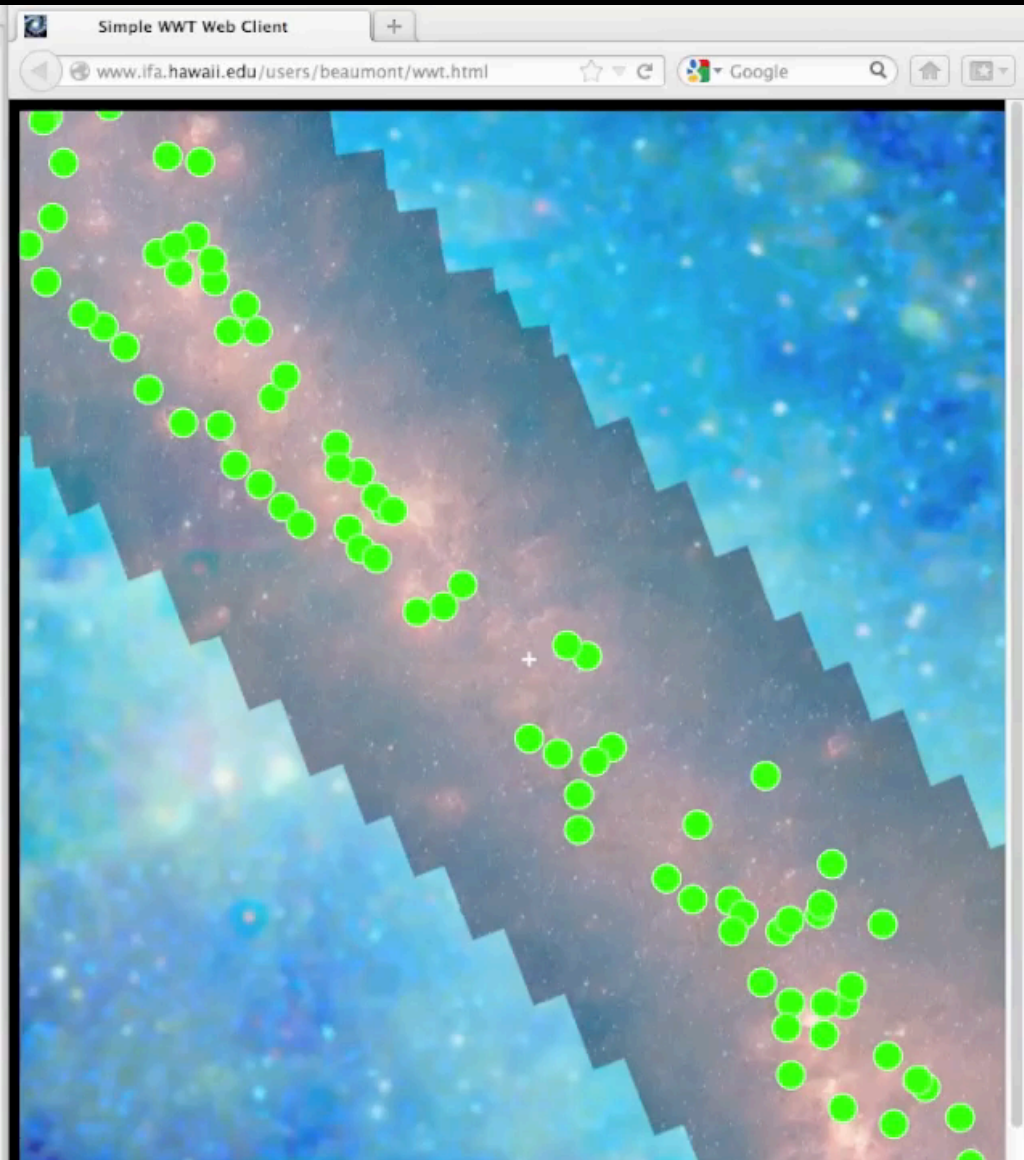
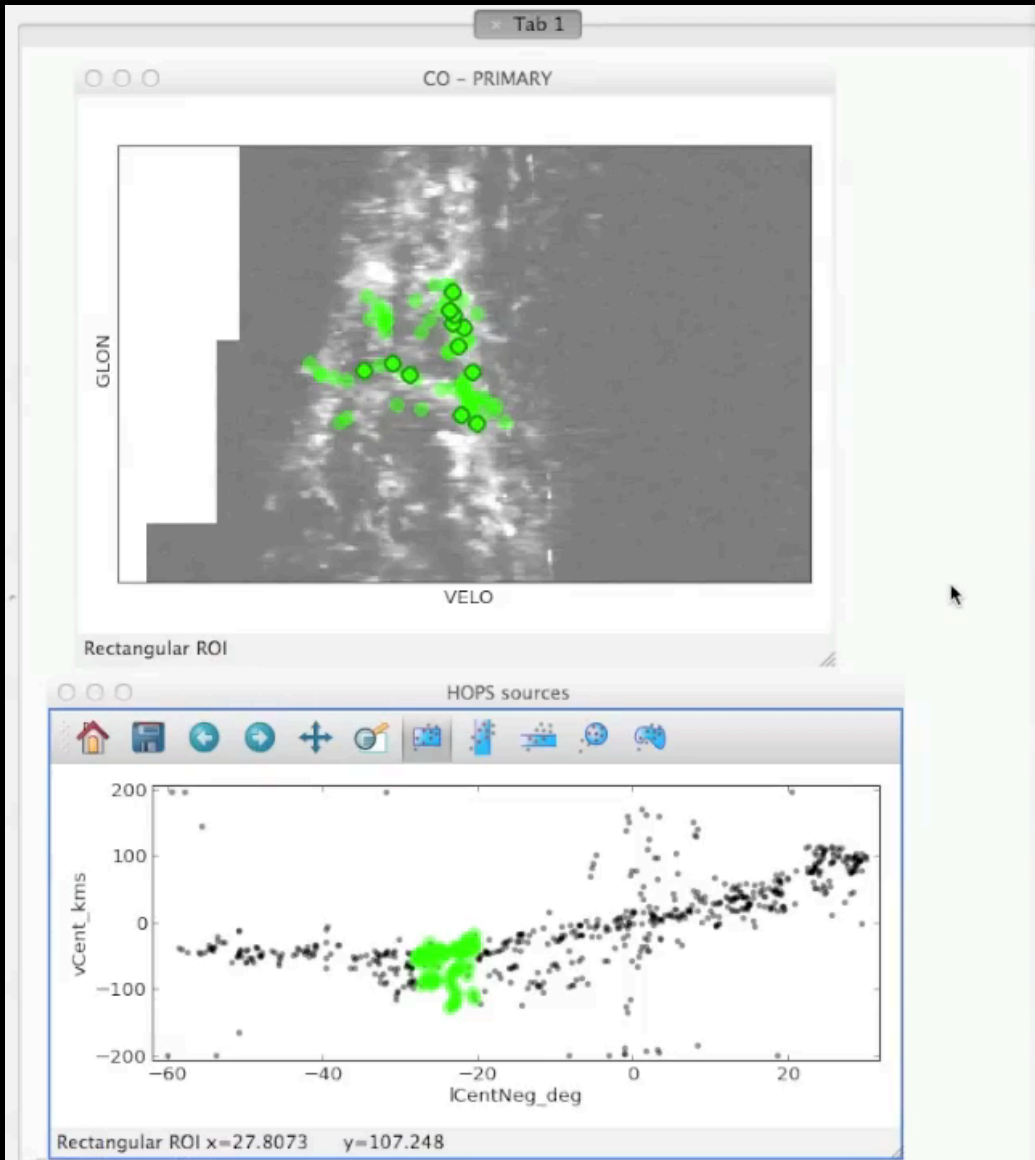
List of Hierarchical Progressive Surveys provided by all public HiPS servers

This page provides the list of all public HiPS sorted by categories, plus the list of the public HiPS servers. It is based on the CDS [MocServer](#) used to aggregate HiPS lists.

HiPS servers (list of HiPS HTTP servers - will required a VO registration in a near future)

<http://aladin.unistra.fr/hips/registry>

#	Origin	Type	HiPS list URL
1	Leiden		http://tgssadr.strw.leidenuniv.nl/hips_list
2	IRAP		http://cade.irap.omp.eu/documents/Ancillary/4Aladin/hipslist-IRAP.txt
3	SSC		http://saada.unistra.fr/cgi-bin/hipslist
4	CDS		http://alasky.u-strasbg.fr/hipslist
5	CDS		http://alaskybis.u-strasbg.fr/hipslist
6	CDS	catalog	http://axel.u-strasbg.fr/HiPSCatService/hiplist
7	AMIGA		http://amiga.iaa.es/hipslist
8	svo.cab		http://gtc.sdc.cab.inta-csic.es/hips/hipslist
9	IAS		http://healpix.ias.u-psud.fr/hipslist
10	ESAC		http://skies.esac.esa.int/hipslist
11	JAXA		http://darts.isas.jaxa.jp/astro/judo2/common/hipslist.cgi



Video courtesy of Chris Beaumont

The "Paper" of the Future

Alyssa Goodman, Josh Peek, Alberto Accomazzi, Chris Beaumont, Christine L. Borgman, How-Huan Hope Chen, Merce Crosas, Christopher Erdmann, August Muench, Alberto Pepe, Curtis Wong

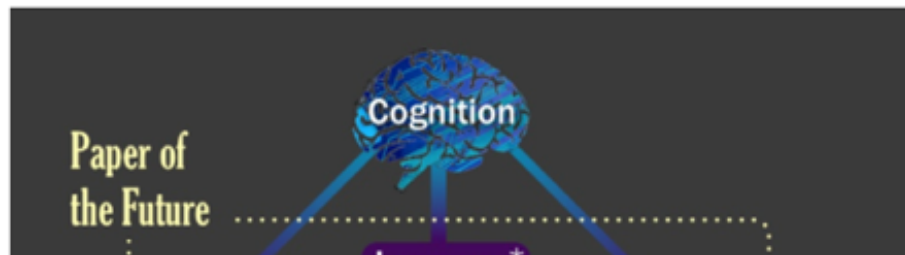
+ Add author ✕ Re-arrange authors

A 5-minute video demonstration of this paper is available at [this YouTube link](#).

1 Preamble

A variety of research on human cognition demonstrates that humans learn and communicate best when more than one processing system (e.g. visual, auditory, touch) is used. And, related research also shows that, no matter how technical the material, most humans also retain and process information best when they can put a narrative "story" to it. So, when considering the future of scholarly communication, we should be careful not to do blithely away with the linear narrative format that articles and books have followed for centuries: instead, we should enrich it.

Much more than text is used to communicate in Science. Figures, which include images, diagrams, graphs, charts, and more, have enriched scholarly articles since the time of Galileo, and ever-growing volumes of data underpin most scientific papers. When scientists communicate face-to-face, as in talks or small discussions, these figures are often the focus of the conversation. In the best discussions, scientists have the ability to manipulate the figures, and to access underlying data, in real-time, so as to test out various what-if scenarios, and to explain findings more clearly. **This short article explains—and shows with demonstrations—how scholarly "papers" can morph into long-lasting rich records of scientific discourse, enriched with deep data and code linkages, interactive figures, audio, video, and commenting.**



3

Konrad Hinsen 3 days ago · Public

Many good suggestions, but if the goal is "long-lasting rich records of scientific discourse", a more careful and critical attitude towards electronic artifacts is appropriate. I do see it concerning videos, but not a word on the much more critical situation in software. Archiving source code is not sufficient: all the dependencies, plus the complete build environment, would have to be conserved as well to make things work a few years from now. An "executable figure" in the form of an IPython notebook wil...

[more](#)

2

Merce Crosas 3 days ago · Public

Konrad, good points; this has been a concern for the community working on reproducibility. Regarding data repositories, Dataverse handles long-term preservation and access of data files in the following way: 1) for some data files that the repository recognizes (such as R Data, SPSS, STATA), which depend on a statistical package, the system converts them into a preservation format (such as a tab/CSV format). Even though the original format is also saved and can be accessed, the new preservation format gua...

[more](#)

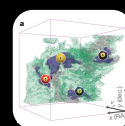
0

Konrad Hinsen 1 day ago · Public

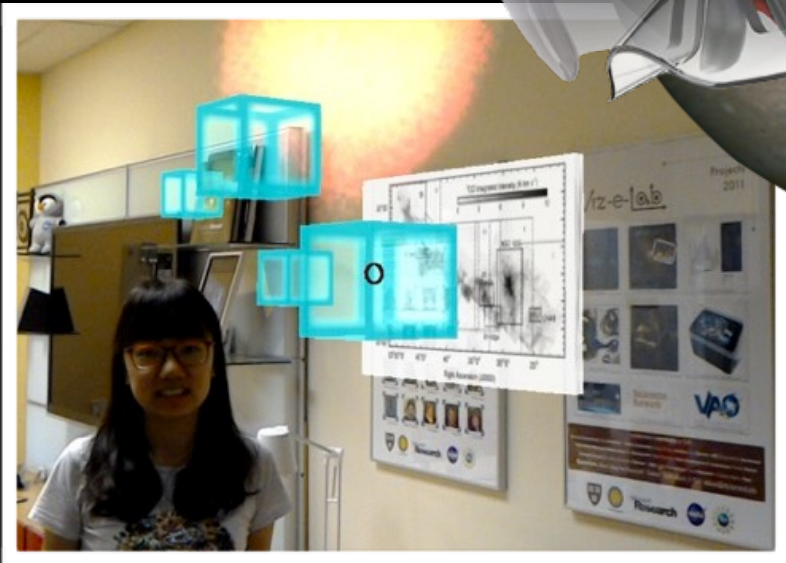
That sounds good. I hope more repositories will follow the example of Dataverse. Figshare in particular has a very different attitude, encouraging researchers to deposit as much as possible. That's perhaps a good strategy to change habits, but in the long run it could well backfire when people find out in a few years that 90% of those deposits have become useless.

Christine L. Borgman 4 months ago · Private

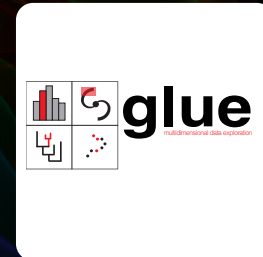
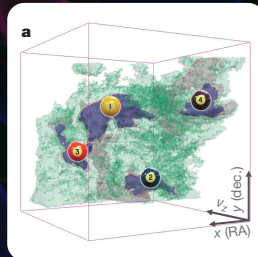
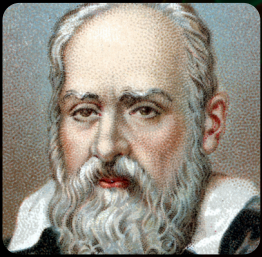
"publications"



WHAT'S NEXT?



THE VALUE OF HIGH-DIMENSIONAL DATA VISUALIZATION IN SCIENCE



Alyssa A. Goodman

*Harvard-Smithsonian Center for Astrophysics
& Radcliffe Institute
@aagie*

Thomas Robitaille

*lead Developer for glue
@astrofrog*

extra slides

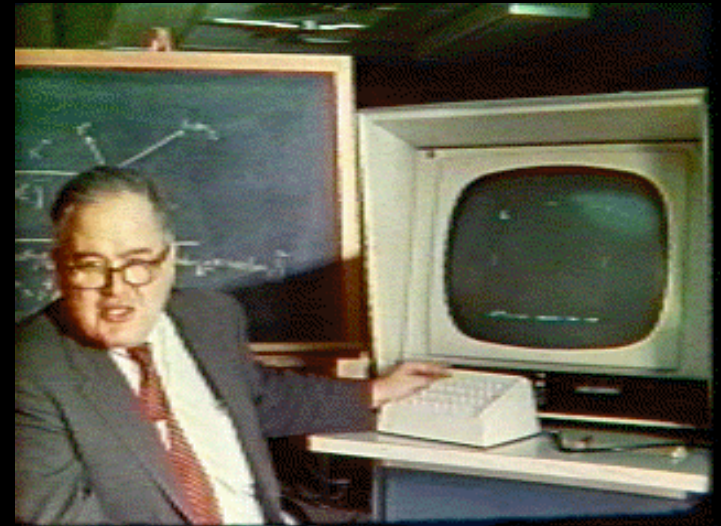


MORE?



[projects.iq.harvard.edu/
seamlessastronomy/
presentations](https://projects.iq.harvard.edu/seamlessastronomy/presentations)

JOHN TUKEY'S LEGACY



PRIM-9

PRIM-H

DataDesk®

XGobi

GGobi

RGGobi

Spotfire®

Polaris

+tableau
SOFTWARE

glue
enhanced & complete

1970

1980

1990

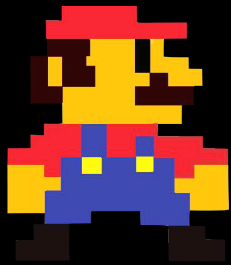
2000

2010

1992



Super Mario Kart: Rainbow Road (1992)



"Today"



Mario Kart 8: Rainbow Road (2014)

